Ecological Indicators 135 (2022) 108559

Contents lists available at ScienceDirect

Ecological Indicators

journal homepage: www.elsevier.com/locate/ecolind

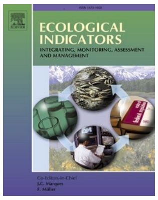

Making the leap from ponds to landscapes: Integrating field-based monitoring of amphibians and wetlands with satellite observations

Elaine M. Brice [a], Meghan Halabisky [b], Andrew M. Ray [c,*]

[a] Department of Wildland Resources, Utah State University, Logan, UT 84322, USA
[b] Conservation Science Partners, Truckee, CA 96161, USA
[c] Greater Yellowstone Network, National Park Service, Bozeman, Montana 59715, USA

ARTICLE INFO

Keywords:
Long-term monitoring
Landsat
Northern range
Greater yellowstone ecosystem
Amphibians

ABSTRACT

A unifying goal of wetland monitoring programs is to characterize how wetland flooding and drying regimes vary in space and time. In remote and mountainous regions, wetlands have been difficult and labor-intensive to monitor, especially at landscape scales. Here, we demonstrate how data from annual, ground-based monitoring of wetlands and amphibians in Yellowstone National Park (YNP) can be enhanced in time and spatial extent by Landsat-based observations of wetlands. Specifically, we applied spectral mixture analysis (SMA) to the Landsat time series to characterize seasonal variation in wetland surface water area over a 35-year period. This extended our monitoring record backward in time (increasing temporal extent) and allowed us to monitor wetlands outside the boundaries of our long-term monitoring catchments, thereby increasing spatial extent. Additionally, we reconstructed and characterized hydroperiod regimes of 427 wetlands across YNP's Northern Range (NR) as ephemeral, intermittent, semi-permanent, and permanent; these categories relate to the local ecology of these sites. Across the NR, the mean summer surface water area in most wetlands declined, regardless of hydrologic regime. Declines in wetland surface water area were associated with variations in snowmelt runoff for approximately half of NR wetlands. The mean effect of runoff on wetland area was strongest for ephemeral wetlands and weakest for permanent wetlands, which were significantly larger than other wetland types. Ground-based observations from established, long-term monitoring sites ($n = 37$) showed that amphibians used all wetland hydroperiod regimes. Intermittent and permanent regime types contained sites where amphibian breeding was consistently detected and highlighted the importance of a portfolio of wetland types for amphibian conservation. Through the integration of ground-based and Landsat satellite datasets, we not only took the leap from ponds to landscapes, dramatically expanding the spatial and temporal extent of monitoring, but also successfully used SMA to characterize hydroperiod regimes and evaluate longer-term wetland surface water area trends across a range of wetland sizes. This work will allow wetland managers to place current conditions within longer-term trends, understand broader patterns of surface water change, analyze the relationship between wetland surface water trends and management actions, and calibrate models of climate impacts. Most importantly, the integration of field assessment and remote sensing technologies offers a strategy to detect changes in wetland extent and condition at scales ranging from individual ponds to landscapes.

1. Introduction

Wetlands, ponds, and other shallow aquatic habitats are increasingly recognized as key ecological indicators from local to global scales (Darrah et al., 2019; Halabisky et al., 2016; Kissel et al., 2020). These keystone habitats are landscape components that disproportionately contribute to biodiversity and resource abundance regardless of their size or distribution (Figel et al., 2019; Locky, 2016; Tews et al., 2004). Wetlands also rank among the most climate-sensitive ecosystems (Matthews, 2010) and consequently serve as leading indicators of climate-induced change. For this reason, monitoring wetland dynamics is increasingly thought to offer prescient knowledge on the ecological manifestations of climate change at local and landscape scales (Kissel et al., 2020; McIntyre et al., 2019; Ryan et al., 2014).

In the U.S. National Park Service's (NPS) Vital Signs Monitoring Program (Fancy et al., 2009; Rodhouse et al., 2016), wetlands and

---

* Corresponding author.
E-mail address: andrew_ray@nps.gov (A.M. Ray).

https://doi.org/10.1016/j.ecolind.2022.108559
Received 1 September 2021; Received in revised form 4 January 2022; Accepted 9 January 2022

wetland-dependent groups (e.g., amphibians) serve as key ecological indicators for tracking the health of >50 national park units (Halstead et al., this issue). While many taxa, including birds, bats, and invertebrates (see Levandowski et al., 2021) are dependent on wetlands, amphibians rank among the most imperiled (Collen et al., 2013; IUCN, 2021) and climate-sensitive vertebrate groups (Case et al., 2015). Many amphibians breed in small, shallow or intermittently flooded wetland habitats. Reliance on wetlands reduces amphibian susceptibility to fish predation and benefits some species' development, but it also increases their vulnerability to climate-induced drying. Moreover, species-specific responses to changes in wetland abundance, depth, and permanence are expected (Hossack et al., 2015, Muths et al., 2017, Ray et al., this issue, Ryan et al., 2014). Unsurprisingly, wetland monitoring programs that are used to inform management actions tend to couple monitoring of physical conditions (i.e., flooding regimes) with biological indicators (e.g., amphibians; see Gould et al., 2019). The former is commonly an afterthought or coupled with ecological monitoring in a way that obscures (due to limited sampling) actual hydrologic dynamics that drive ecological patterns, while the latter offers inimitable understanding of past and future wetland change (Hossack et al., 2017, Ray et al., 2019, Walls et al., 2013).

A unifying goal of most wetland and amphibian monitoring programs is to characterize how wetland flooding and drying regimes vary in space and time (Halabisky et al., 2016). For example, McMenamin et al. (2008; n = 49) used point-in-time monitoring and Schook and Cooper (2014; n = 24) used automated loggers to continuously monitor hydrologic dynamics in a relatively small number of wetlands across northern regions of Yellowstone National Park (YNP), USA. In contrast, the NPS's ongoing Vital Signs Monitoring Program (Ray et al., 2016) uses a stratified, random monitoring design and annual, ground-based visits to >300 wetland sites across Yellowstone and Grand Teton national parks (combined area ~10,300 km^2). While the aforementioned monitoring approaches reveal information on the dynamics or permanence of individual wetland hydroperiods, there is growing interest in the thoughtful integration of ground-based data with remotely sensed observations to increase the frequency of wetland observations (Halabisky et al., 2016; Pasquarella et al., 2016). This combination of data sources, with their complementary spatial and temporal resolutions and extents, make it possible to better capture links between wetland hydrologic regimes and biological groups that are dependent on wetlands for elements of their life cycle (Kissel et al., 2020).

When paired with ground-based monitoring and its many benefits (e.g., ground-truthed, site-specific data), remote sensing technologies provide additional spatiotemporal detail that extends out in space and back in time. For example, the Landsat archive allows managers to retrospectively describe dynamics of habitat change since 1984 and offers significant insight on multi-decadal trends at wetlands of significant interest (Halabisky et al., 2016; Sall et al., 2021). Importantly, when these datasets are combined with climate or water balance estimates, it provides opportunities to evaluate the drivers of wetland change (Lee et al., 2015; Ray et al., 2019) and characterize the idiosyncratic responses of individual wetlands within larger landscapes (Halabisky et al., 2016; Kissel et al., 2020). Finally, remote sensing information provides opportunities to apply a standardized and modern classification process for describing the hydrologic regime of wetlands across large or remote geographic locations (Gallant, 2015).

In wetlands, the hydroperiod, or pattern of flooding and drying, is the most important driver in the establishment and maintenance of specific habitat types (Cowardin et al., 1979), and determines which plant communities or species are present (Casanova and Brock, 2000; Tarr et al., 2005). This biological filter also applies to invertebrates, amphibians, and waterfowl (Wellborn et al., 1996). Even modest departures from historic hydroperiods (driven by climate change or land use impacts) could limit future availability of these habitats to wetland dependent species. To inform management of climate-sensitive wetland resources, long-term ecological monitoring programs tasked with characterizing wetland hydroperiods must consider approaches that model within-year peculiarities of individual wetland hydroperiods and integrate that information with spatially-linked monitoring of biological indicators (McIntyre et al., 2019).

Long-term vital signs monitoring programs in U.S. national parks have been simultaneously monitoring wetlands and amphibians across large, relatively pristine landscapes, providing unique opportunities to evaluate strategies to integrate remote sensing datasets. To date, ground-based monitoring datasets from YNP and Grand Teton National Park (GTNP) have documented annual conditions of wetlands (wet or dry at time of visit) and associated amphibian breeding activity and offered insight on how annual drying of wetlands affects breeding by multiple amphibian species (Gould et al., 2019; Ray et al., 2016). In these parks and others across the western U.S., climate change is affecting wetlands in subtle ways that may go undetected from single, ground-based observations of wetlands each year. Remote sensing techniques are well-suited for characterizing subtle changes to the hydroperiods of wetlands and provide greater power for detecting changes to hydroperiods that are not possible from shorter monitoring records based on a single observation made each year (Rowe et al., 2021).

The aim of this case study was to blend point-in-time observations of wetland flooding status and amphibian use of individual sites with Landsat-derived seasonal summaries of wetland surface water area. We then applied these methods to describe wetland hydrologic regimes and characterize trends in wetland surface water area for an entire landscape. We used data from an NPS long-term monitoring dataset (2005 to 2019) and from catchments (i.e., clusters of wetlands) surveyed across YNP's Northern Range (Fig. 1).

Our approach applied spectral mixture analysis (SMA; Halabisky et al., 2016) of a Landsat time series (1984 to 2018) to construct multi-decadal hydroperiods for each long-term monitoring site. We used these hydroperiod reconstructions of the past and present to categorize the hydrologic regime (ephemeral to permanent) and describe trends in surface water area for each focal wetland (n = 37). Next, we leveraged our 15-year amphibian monitoring dataset for these same wetlands to test whether amphibian breeding could be discriminated by hydrologic regime. To evaluate how these long-term monitoring sites represented the larger population of sites in YNP's Northern Range (NR), we applied these same methods to NWI-mapped palustrine and lacustrine habitats across the NR (n = 427). For NWI-mapped wetlands, we characterized the hydrologic regime using widely recognized narrative descriptions from Cowardin et al. (1979) and documented surface water area trends during snow-free periods (15 May to 15 October each year). In addition, we explored relationships between snowmelt runoff, a water balance derivative linked to wetland drying (Ray et al., 2019), and June surface water area trends using this same time series (1984 – 2018). Finally, we describe the sensitivity of the relationship between June wetland surface water area and runoff and identify ecological pivot points (*sensu* Thoma et al., 2019), or the amount of runoff needed for a wetland to be maintained at its long-term mean size. We conclude with recommendations on how these datasets can be further integrated into the ongoing monitoring program in YNP and GTNP.

2. Materials and methods

2.1. Study area

The NR is a 1400 km^2 region characterized by relatively flat, glaciated valleys surrounded by mountains. Low elevations are dominated by grassland and sagebrush steppe communities and coniferous forest predominates at higher elevations. The NR represents portions of the upper Gardiner, Lamar, and Yellowstone River watersheds and extends across northwestern Wyoming and southern Montana, USA and within and outside of YNP (Fig. 1; Ripple et al., 2001). The NR is recognized as a hotspot for ungulate diversity (Mosley et al., 2018) and the landscape

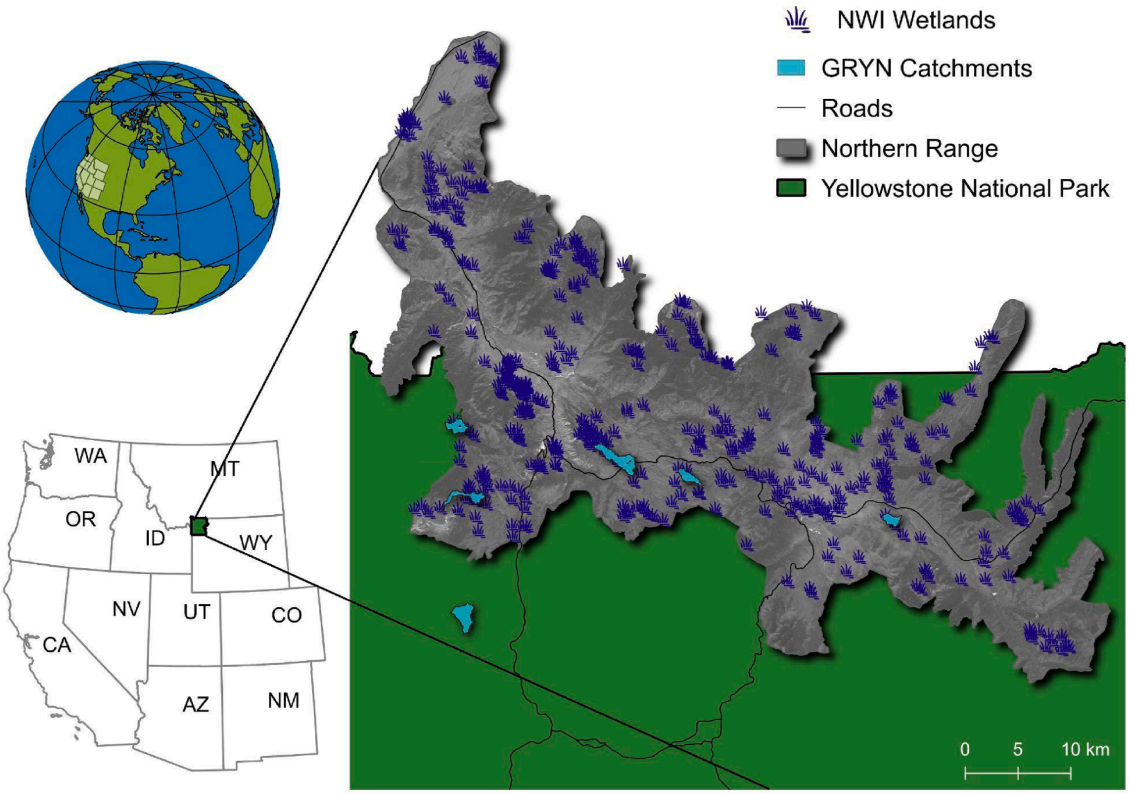

Fig. 1. Location of the Northern Range (NR) and Yellowstone National Park (YNP), USA. The NR is a 1400 km^2 region that extends across northwestern Wyoming and southern Montana. The National Park Service's Greater Yellowstone Network (GRYN) has been monitoring clusters of wetlands in six catchments in or adjacent to the NR since 2005 (n = 37). US Fish and Wildlife Service National Wetland Inventory (NWI) mapped wetland (palustrine and lacustrine) locations are also shown (n = 427).

contains high densities of depressional wetlands (Schook and Cooper, 2014). The NR's lower elevation, large rivers, and abundance of non-forested wetlands distinguish it from other portions of YNP.

There are four native amphibian species found across the NR: western tiger salamander (*Ambystoma mavortium*), western toad (*Anaxyrus boreas*), boreal chorus frog (*Pseudacris maculata*), and Columbia spotted frog (*Rana luteiventris*). All species have complex life histories and require water for breeding and larval development before metamorphosing. The species range from highly aquatic (Columbia spotted frogs) to more terrestrial (western toads) and from longer (≥12 years for western toads and spotted frogs) to shorter (3 to 5 years for chorus frogs) life spans. Spotted frogs and chorus frogs typically metamorphose within 2 to 4 months in the same summer that eggs are deposited. Western tiger salamanders are longer-lived species and salamander larvae may complete metamorphosis in one season, or, at higher elevations, overwinter as larvae. Alternatively, in deep, permanent wetlands, salamanders can reach sexual maturity in their paedomorphic or water-dependent larval form (Koch and Peterson, 1995). Western toads, the least common of the four species, have larval development periods that range from 1 to 2 months (Turner, 1955).

2.2. *Ground-based monitoring*

We monitored amphibians at 37 wetlands across six catchments in northern YNP from 2005 – 2019. These wetlands are part of a random sampling framework that was established in 2005 and continues to this day. This framework randomly selected catchments from four major subbasins across YNP (Gould et al., 2012, Ray et al., this issue); the NR represents one of these four subbasins. All wetlands, ponds, and small lakes within selected catchments that contained standing water for amphibian breeding were sampled each year; the 37 wetlands from the NR represent approximately 15% of surveys conducted annually as part of our larger annual vital signs monitoring program in YNP (Ray et al., this issue). In dry years, we documented the absence of water in wetlands. Surveys were conducted from early June through July and varied depending on elevation. Visual encounter surveys were timed to detect evidence of breeding activity (i.e., larvae and metamorphs) by species using dip nets; surveys were conducted by two independent observers during a single-site visit (see Gould et al., 2012).

To access Landsat satellite imagery for each long-term monitoring site, we delineated wetland boundaries in QGIS through manual photo interpretation of multiple public imagery datasets (e.g., NAIP, Digital Globe) available through ESRI and Google. Specifically, we drew polygons (i.e., boundaries) that captured all visible water, as well as dry areas within the high-water level (i.e., maximum surface water elevation) of each wetland basin (Schook and Cooper, 2014). The high-water level is commonly visible on imagery as the location where natural vegetation changes; on the ground this represents a change from predominantly aquatic to predominantly upland vegetation. We established the high water level by examining imagery provided through Google Earth of each wetland through time. Furthermore, we added a 5-m buffer to ensure we captured the maximum surface water elevation for each wetland and corrected for any spatial misalignment between image datasets, while still avoiding overlap with neighboring wetlands. We then used these same polygons in spectral mixture analysis (SMA; Halabisky et al., 2016) to estimate surface water area from 1984 to 2018 (see methods below) for each wetland.

Using years 2005–2019 of amphibian monitoring and wetland data from ground-based surveys, we used a Chi-square test of independence to examine whether cumulative amphibian species richness (summarized as the total richness of species documented breeding at a site across all years) was independent of wetland hydrologic classifications (ephemeral, intermittent, semi-permanent, and permanent; see below). Cumulative species richness ranged from zero to four across sites. Due to small sample sizes, we pooled sites based on species richness into two groups: zero or one species detected across all years and ≥ 2 or more, to maintain the test distribution approximation.

To determine if amphibian breeding occurrence differed among wetland types, we computed the percentage of breeding occurrence for each wetland site over the 15-year survey period; note that not all sites were monitored in all years. A Kruskal-Wallis nonparametric test was used to compare differences in percent breeding occurrence while adjusting for ties among the ranked observations (Hollander and Wolfe, 1999).

2.3. Wetland delineation of NWI-mapped wetlands

We accessed the U.S. Fish and Wildlife Service (FWS) National Wetland Inventory (NWI) from the online data mapper (www.fws.gov/wetlands/data/mapper.html) in May 2019 and downloaded a shapefile of wetland polygons that fell within the boundary of the NR (watersheds HU810070001 and HU810070002). Since a major goal for this study was to evaluate surface water area change in the primary amphibian habitats within the NR, we removed any narrow riverine (streams and rivers) wetlands that were wholly associated with flowing waters (amphibians in our region do not breed in flowing water). We merged all palustrine wetland polygons classified as: PEM, PAB, PUB, and PUS; Cowardin et al., 1979) that shared a boundary and added a 5-m buffer to each individual polygon (isolated and merged). This cleaning process reduced the NWI shapefile from 3956 to 2845 polygons. We then selected all polygons that the NWI classified as palustrine wetlands [class types: PAB, PUB, and PUS] or lakes [L1AB and L1UB], resulting in 429 wetland polygons ranging in size from 285 m^2 to 1,347,132 m^2.

From a visual inspection of the NWI polygons overtop satellite imagery, many NWI-mapped wetlands misrepresented wetlands detected on imagery and identified by vegetation ecotones or the presence of water. Some NWI-mapped wetland boundaries were under- or over-represented relative to conditions observed on aerial imagery, while others were offset from the wetland (see Appendix, Fig. A1). Others were missing the wetland entirely. Due to these issues, we manually digitized boundaries for 427 distinct NWI wetlands based on satellite imagery provided with ESRI software and through Google.

2.4. Landsat-derived estimates of wetland surface water area

Using the Google Earth Engine platform, we reconstructed changes in surface water area for each of the 427 palustrine wetlands and small lakes as well as the 37 established, long-term monitoring sites described above using an SMA model of a time-series of Landsat 5 Thematic Mapper and Landsat 8 OLI Level 1 satellite image scenes hosted by USGS (https://www.usgs.gov/landsat-missions/data) and spanning years 1984 – 2018. Landsat 8 products were atmospherically corrected using the Land Surface Reflectance Code (LaSRC) (Vermote et al., 2016) and Landsat 5 products were atmospherically created using the LEDAPS algorithm by Google in Google Earth Engine (Masek et al., 2012).

We included only snow-free images from May 15th to October 15th each year, where cloud cover composed <40% of the image scene and converted the Landsat imagery time-series into estimates of surface water area (see Kissel et al., 2020) using the constrained four-endmember SMA model described in Halabisky et al. (2016). SMA uses the spectral signatures of the dominant physical scene components (e.g., water, trees, grassland), called endmembers, to estimate the fractional cover of each endmember for every pixel in the image scene (Fig. 2). As a result, SMA provides estimates of each scene component at sub-pixel scales. Endmembers represent “pure” pixels where 100% of the pixel is composed of a single physical feature (e.g., water). For our SMA model we selected four “image” endmembers of the physical scene components (i.e., water, wetland vegetation, trees, and grassland) using

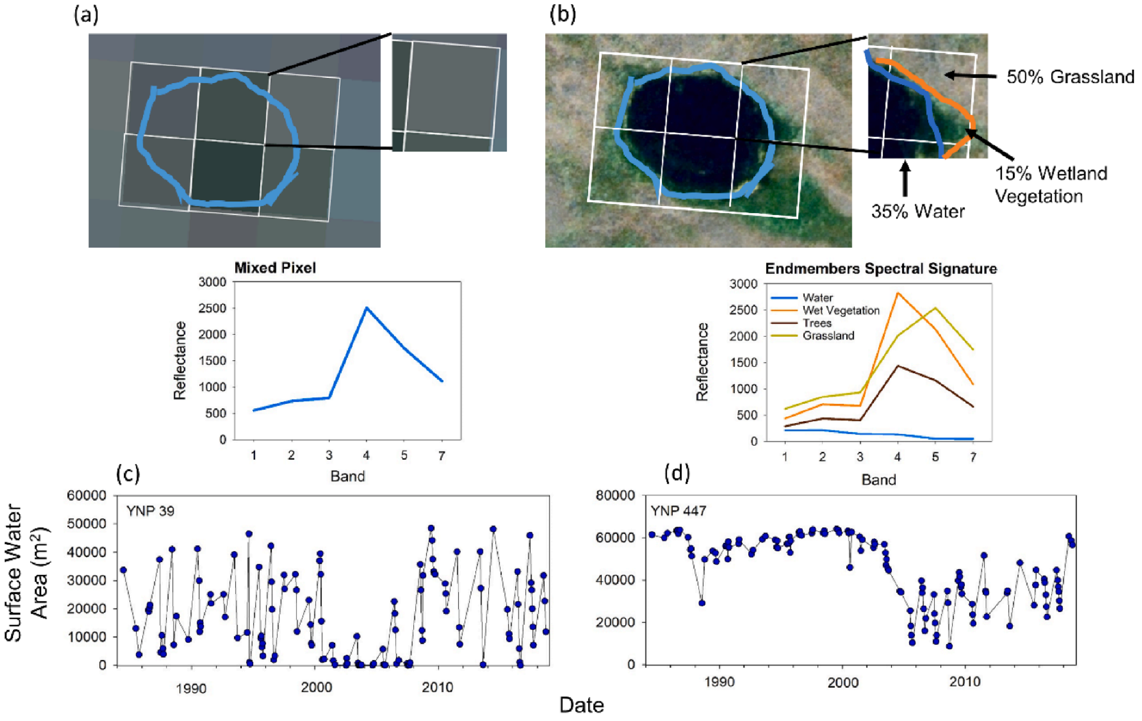

Fig. 2. (a) Schematic of a Landsat image (as part of a series spanning 1984 – 2019) for an individual wetland, where the chart represents the “mixed” signature of the zoomed pixel. (b) Spectral mixture analysis uses the spectral signature of the endmembers (represented by the small plot) to estimate the proportion of each land class feature in the “mixed” pixel. The wetland polygon is shown here with a high-resolution aerial image to illustrate the land-cover components within a mixed pixel. (c and d) Examples of a time-series of wetland surface water area estimates for two wetlands in our study system. Note both wetlands experienced a reduction in surface water area during the multi-year drought of the early 2000s (2000–2007) and recovery post drought. Basemap source: ArcGIS World Imagery basemap; ESRI.

on-the-ground knowledge of the study area. We identified endmembers for water, grassland, and trees for each image in the time-series. Pure pixels for wetland vegetation were not available for each image in the time-series; therefore, we created endmembers for wetland vegetation from a mean composite of known wetland vegetation locations on the ground for the entire time-series. This technique allowed us to create scene-specific SMA models to reduce the impacts of atmospheric noise and sensor differences between Landsat 5 and Landsat 8, and provided a fractional estimate of surface water for each pixel ranging from zero to one for each image in the Landsat time-series. The product of the fractional estimate for each pixel and the area of a Landsat pixel (30 m × 30 m or 900 m^2) was used to generate surface water area estimates in square meters for each pixel in the image scene (see Fig. 2).

To create a time-series of wetland-specific surface water area, we buffered our field-delineated wetland polygons by 5 m (see above) to compensate for variations in wetland surface water area that had not been documented during field visits or represented on reference imagery. This buffer distance was used previously (see Kissel et al., 2020) and it reduced issues from potential misregistration between Landsat scenes, addressed the issue of underestimating wetland area in high water years, and prevented the unintentional inclusion of visible water from neighboring wetlands.

We validated our SMA model using linear regression comparing two reference datasets (see Appendix, Table A1, Fig. A2) created from ground-based and imagery-based delineations of surface water with our SMA Landsat-derived surface water estimates. Ground-based delineations were completed on a subset of wetlands (27 wetlands chosen for their accessibility and spread geographically across the NR representing 50 total observations) in June and July of 2018 and 2019. The SMA estimates were highly correlated with the ground-based estimates (Spearman's $r = 0.89$, $R^2 = 0.85$; Fig. A2). To increase our validation sample size and extend our coverage, we also estimated the amount of surface water area in all 427 wetlands using Planet imagery (4-m resolution) available from June 3, 4, and 6 and August 3, 2017. For validation, we only used delineations within 10 days of a Landsat scene for our regression model (Kissel et al., 2020). Redrawing the NWI wetland polygons increased the fit between Planet imagery and SMA for all wetlands (from $R^2 = 0.73$ to $R^2 = 0.78$), but even more so for smaller (<1000 m^2) wetlands (from $R^2 = 0.16$ to $R^2 = 0.47$; Table A1, Fig. A2). This increase in fit indicates that redrawing the NWI polygons more accurately captured the true extent of each wetland, thereby improving the predictive ability of SMA surface water area.

2.5. *Categorization of hydrologic regime*

For both sets of wetlands (established NPS long-term monitoring sites and NWI-mapped), we classified wetland hydrologic regimes into four distinct types (ephemeral, intermittent, semi-permanent, and permanent) following descriptions from Cowardin et al., (1979) and based on annual frequency of drying. While Cowardin et al. (1979) applied categories using narrative criteria, other data-rich studies (see McCaffery et al., 2014; Richter-Boix et al., 2007; Snodgrass et al., 2000; Walls et al., 2013 as examples) and our case study expanded on these narratives and applied numeric thresholds to classify hydroperiods present within our study area.

For each wetland, we calculated the 95th percentile of surface water area estimated from the SMA and used this value as the maximum wetland size. We did not use the true maximum to prevent the use of extreme outliers. For each SMA observation (i.e., multiple per year), we converted wetland surface water area to percent of the maximum. Wetlands that were 10% or less of the maximum area were defined as "dry"; we used 10% as the cut-off rather than true 0 to account for error in the SMA model (Kissel et al., 2020). If at least one observation during the year was dry, that year was considered dry. We then calculated the proportion of dry years for each wetland. Consistent with hydrologic types described by Cowardin et al. (1979) wetlands that had regimes characterized as dry for $\leq 5\%$ of years were classed as permanent, wetlands dry for $> 5\%$ and $\leq 25\%$ of years were classed as semi-permanent, wetlands dry for $> 25\%$ and $\leq 75\%$ of years were classed as intermittent, and wetlands that were dry for $> 75\%$ of years were classed as ephemeral.

2.6. *Surface water trends in Northern Range wetlands*

Using the SMA estimates of surface water area, we analyzed trends in wetland surface water area over time for both sets of wetlands (ground-based $n = 37$, NWI-mapped $n = 427$). For each wetland, we used the average of all snow-free (May 15 to October 15) dates of estimated wetland surface water area and scaled them to have a mean of 0 and standard deviation of 1. We ran a linear regression of the scaled area as a function of year (observations ranged from 50 to 140 among wetlands) over the 35-year Landsat time series. Models included an autoregressive correlation structure to account for temporal autocorrelation. Using scaled surface water area allowed us to directly compare the rates of surface water area change across wetlands. We used linear regression for individual wetlands rather than fitting a linear mixed model with an individual wetland identifier as a random effect because mixed models including a random slope for each wetland failed to converge. We compared the mean slopes of wetland surface water area change over time using hydrologic regime as a grouping variable and ANOVA and Tukey's Honest Significant Difference (HSD) Test.

2.7. *Runoff as a driver of wetland dynamics*

We modeled June wetland surface water area as a function of water year (October to September) runoff to determine the extent to which NR wetlands (ground-based and NWI-mapped) are driven by variations in this climate driver. We focused our analysis on June surface water area because most NR wetlands are near their annual maximum in June (Schook and Cooper, 2014), and used runoff because it has been shown to be strongly associated with wetland inundation across YNP (Gould et al., 2019; Ray et al., 2019). We calculated runoff from a Thornthwaite-type monthly water balance model (Tercek et al., 2021, Thoma et al., 2015) and used annual water year estimates of runoff to evaluate variations in June wetland surface area. We ran linear models of scaled June surface water area as a function of water year runoff. We again included an autoregressive correlation structure to account for temporal autocorrelation, used an individual model for each wetland to determine whether the effect of runoff on wetland area varied by hydrologic regime, and compared mean slopes of each type with an ANOVA and Tukey's HSD Test.

2.8. *Wetland sensitivity and ecological pivot points*

Finally, we evaluated the sensitivity of June surface water area of wetlands (ground-based and NWI-mapped) to variations in annual water year runoff and identified the ecological pivot point for each wetland. Pivot points are the amount of water year runoff needed to maintain a wetland's water level at its long-term (1984–2018) mean surface area (Thoma et al., 2019). With runoff below the pivot point value, June wetland surface water area falls below its mean and with runoff above the pivot point value, wetland surface water area swells above its mean size. We further summarized pivot points by hydrologic groups and compared means with an ANOVA and Tukey's HSD Test.

3. Results

3.1. *Long-term, ground-based monitoring sites*

Between 2005 and 2019, we visited 37 wetlands from six NR catchments representing a total of 505 site visits. These ground-based surveys revealed variations in wetland drying and amphibian breeding among wetland sites and years (Figs. 3 and 4). Some wetlands (e.g., 955–2 and 955–6; Fig. 3) supported amphibian breeding each year. Others contained standing water each year, yet amphibian breeding was never detected (e.g., 4007–71). Species' use of individual wetlands also varied across space and time: the maximum number of four species was detected breeding within a single site and single year on just four occasions. Three species were detected breeding during 34 site-year occasions, two species on 104 occasions, and one species on 127 occasions; no breeding was recorded on 236 (47%) of the 505 total site-visits. Despite this finding, most wetlands (81%) included in the annual ground-based monitoring program supported at least one breeding species over 15 years of monitoring.

Boreal chorus frogs were the most common species detected breeding across monitoring sites. Tiger salamander breeding was also common across NR catchments and in two catchments breeding by this species predominated. Spotted frog breeding was common at some sites and particularly within catchments at elevations >2300 m. In these catchments, spotted frog occurrence was associated with larger wetlands. Although widespread in their occurrence, western toad breeding was less common and detected in only three of the six NR catchments over 15 years.

To expand the temporal extent of our annual, single-visit observations of long-term monitoring sites and examine longer-term trends, we applied Landsat-based observations to these 37 wetlands. Landsat-derived estimates of surface water area for monitoring sites showed that mean wetland surface area over the 35-year time series varied by several orders of magnitude ($\mu = 6810$ m^2; range = 18–74,158 m^2). The estimated proportion of years dry (derived from satellite observations) also varied among monitoring sites (range 0 to 1) and was inversely correlated with mean surface water area ($r_s = -0.635$, $p < 0.01$) and site elevation ($r_s = -0.349$, $p = 0.03$). The percentage of years with documented amphibian breeding (regardless of species) was also positively correlated with wetland area ($r_s = 0.338$, $p = 0.04$).

3.1.1. *Categorization of hydrologic regimes*

Most (70.2%) of the long-term monitoring sites were classified as either ephemeral ($n = 12$) or intermittent ($n = 14$; Table 1 and Fig. 5a and b), indicating that these sites frequently (ephemeral) or regularly (intermittent) dry or shrink to below 10% of their maximum area before 15 October. Only one site had a hydroperiod that satisfied the semi-permanent criteria (Table 1). Amphibian breeding was detected in all hydrologic types (ephemeral to permanent) but not all wetlands (Figs. 3 and 5c and d). The proportion of years over our 15-year times series that amphibian breeding was documented at a site did not differ by wetland hydrologic type ($H = 0.072$; $p \approx 0.96$ based on a chi-square distribution with 2 df; Fig. 5d); however, breeding occurrences ranged between 46% for permanent and semi-permanent sites to 58% for intermittent sites. Intermittent (5 sites) and permanent (1 site) hydrologic types contained the only examples where breeding was detected at a site in all years. Of the 505 site-visits, breeding occurred in intermittent wetlands ($n = 14$) on 118 occasions compared with 79 occasions for ephemeral ($n = 12$) and 62 occasions for permanent ($n = 10$) wetlands. There was no observable difference in amphibian species richness among wetland hydrologic types ($\chi2 = 0.204$; $p = 0.90$; df = 2; Fig. 5c). We detected one or fewer species over all survey years for 12 of the 37 sites. The remaining 25 sites consisted of 14 sites with two species, 10 sites with three species and one site with four species detected. Some wetlands, regardless of hydrologic type, consistently supported more breeding species than others (see Fig. 3 for examples). Those that dried regularly still supported breeding in years where there was sufficient snowmelt runoff to fill and retain water through the breeding season. As an example, site 4007–3 supported breeding by multiple amphibian species despite being completely dry in early July 2005, 2006, 2007, 2010, 2013, and 2016 (see Figs. 3 and 4).

3.1.2. *Surface water trends over time*

Most (75.7%, $n = 28$) of the 37 wetlands visited each year experienced a decrease in surface water area from 1984 to 2018 (Fig. 6a), although only 13 wetlands (35.1%) experienced a significant change over time (Fig. 6a). On average, intermittent wetlands exhibited the greatest decrease in surface water area ($\mu\beta \pm SE = -0.031 \pm 0.010$), followed by permanent wetlands (-0.015 ± 0.011) and ephemeral

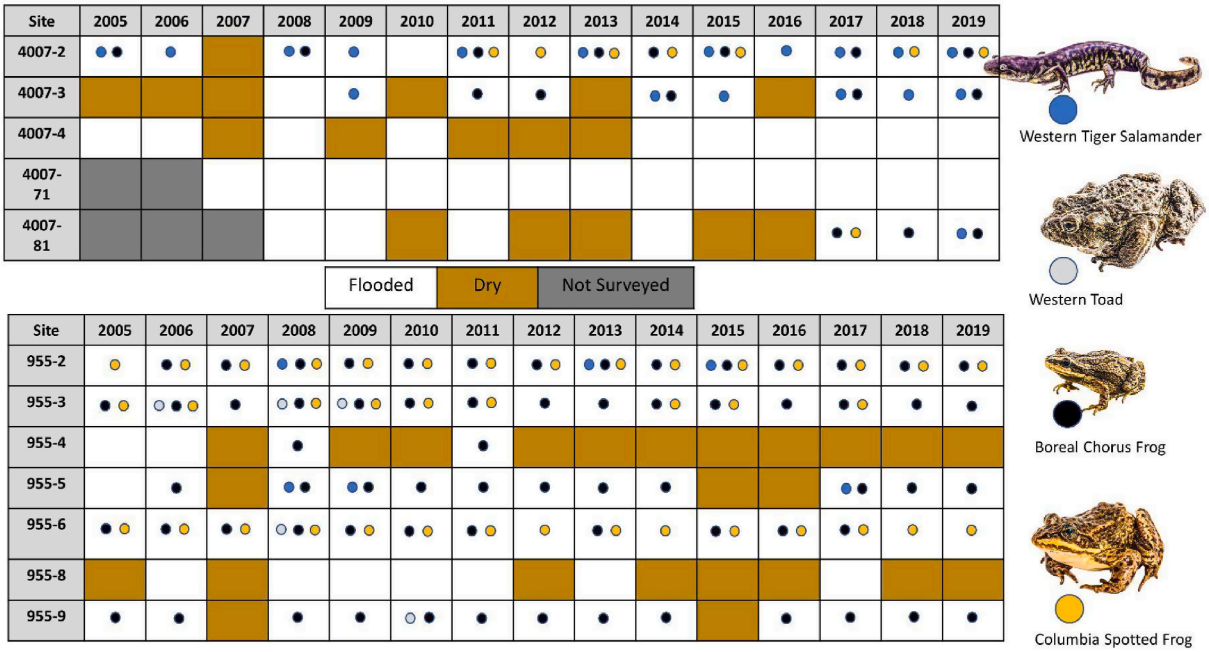

Site	2005	2006	2007	2008	2009	2010	2011	2012	2013	2014	2015	2016	2017	2018	2019
4007-2	🔵⚫	🔵	🟫	🔵⚫	🔵		🔵⚫🟠	🟠	🔵⚫🟠	⚫🟠	🔵⚫🟠	🔵	🔵⚫	🔵🟠	🔵⚫🟠
4007-3	🟫	🟫	🟫		🔵	🟫	⚫	⚫	🟫	🔵⚫	🔵	🟫	🔵⚫	🔵	🔵⚫
4007-4			🟫		🟫		🟫	🟫	🟫						
4007-71	▨	▨													
4007-81	▨	▨	▨			🟫		🟫	🟫		🟫	🟫	⚫🟠	⚫	🔵⚫

Flooded	🟫 Dry	▨ Not Surveyed

Site	2005	2006	2007	2008	2009	2010	2011	2012	2013	2014	2015	2016	2017	2018	2019
955-2	🟠	⚫🟠	⚫🟠	🔵⚫🟠	⚫🟠	⚫🟠	⚫🟠	⚫🟠	🔵⚫🟠	⚫🟠	🔵⚫🟠	⚫🟠	⚫🟠	⚫🟠	⚫🟠
955-3	⚫🟠	⚪⚫🟠	⚫	⚪⚫🟠	⚪⚫🟠	⚫🟠	⚫🟠	⚫	⚫	⚫🟠	⚫🟠	⚫	⚫🟠	⚫	⚫
955-4			🟫	⚫	🟫	🟫	⚫	🟫	🟫	🟫	🟫	🟫	🟫	🟫	🟫
955-5		⚫	🟫	🔵⚫	🔵⚫	⚫	⚫	⚫	⚫	⚫	🟫	🟫	🔵⚫	⚫	⚫
955-6	⚫🟠	⚫🟠	⚫🟠	⚪⚫🟠	⚫🟠	⚫🟠	⚫🟠	🟠	⚫🟠	🟠	⚫🟠	⚫🟠	⚫🟠	🟠	🟠
955-8	🟫		🟫					🟫		🟫	🟫	🟫		🟫	🟫
955-9	⚫	⚫	🟫	⚫	⚫	⚪⚫	⚫	⚫	⚫	⚫	🟫	⚫	⚫	⚫	⚫

Fig. 3. Summary of ground-based survey results for National Park Service's long-term monitoring sites associated with two Northern Range catchments. Wetland sites are shown on the left of the matrix for catchments 4007 and 955 and years 2005 to 2019. Brown fill indicates the site was dry when visited in July of that year. White fill indicates water was present and circles indicate breeding was detected, where Western Tiger Salamanders are blue, Western Toads are silver, Boreal Chorus Frogs are black, and Columbia Spotted Frogs are orange. If a site was not visited in a given year, that cell is grayed (e.g., 4007-71 in 2005).

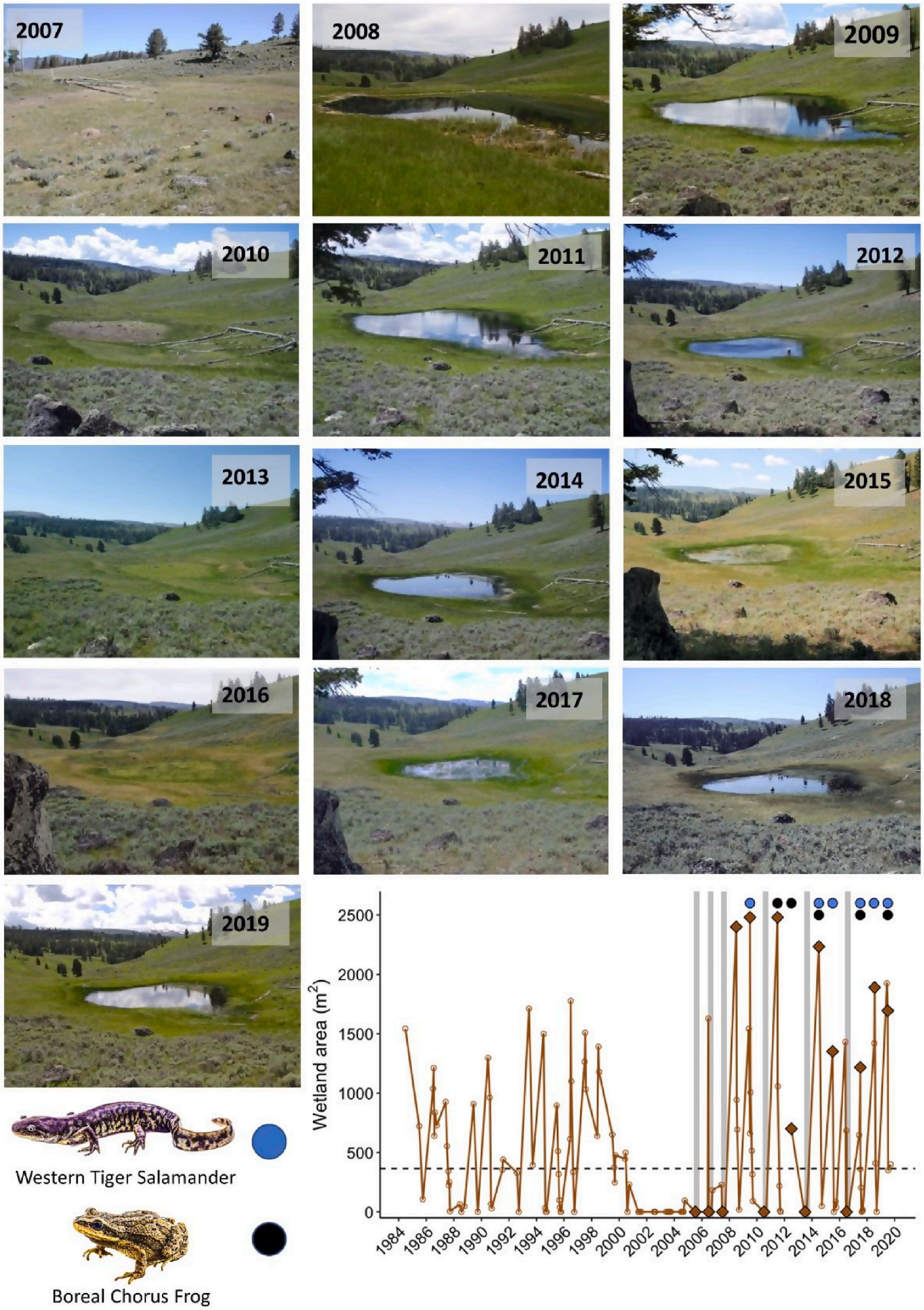

Fig. 4. Photographs of annual wetland visits to an isolated wetland (Y4007-3) in Yellowstone's Northern Range. This wetland was dry during early July sampling visits in 2005, 2006, 2007, 2010, 2013, and 2016. The hydrograph in the lower right shows the Landsat-based reconstruction of this site's hydrograph dating back to 1984. Ground-based wetland area estimates (brown diamonds) were used to supplement spectral mixture analysis (SMA) estimates of wetland surface water area. Dry visits observed through annual visits are shown as silver bars. Species detected during surveys are shown using multi-colored circles: Western Tiger Salamanders (blue) and Boreal Chorus Frogs (black). The long-term mean wetland surface water area used to identify the ecological pivot point (see methods) is shown with a dashed line.

Table 1
Summary of wetland hydrologic types for the National Park Service's long-term monitoring sites. The table includes the number of wetlands (N), group mean of the individual wetland elevation and mean area by hydrologic regime (Mean, μ [± SE]), and mean of the 95th quantile (95th Q, μ [± SE]) area for all wetland hydrologic regimes. In addition, the proportion of years of amphibian breeding was detected (mean and range) and the cumulative richness of amphibian species (median and range) are shown.

Wetland Type	N	Elevation (m)	Mean Area (m^2)	95th Q Area (m^2)	Prop. Yrs Breeding	Amphibian Richness
Ephemeral	12	2208.0 (±41.6)	528.2 (±259.7)	2518.7 (±973.2)	0.49 (0.00 – 0.93)	2 (0 – 3)
Intermittent	14	2299.7 (±34.1)	2219.8 (±1171.9)	6713.6 (±3220.1)	0.59 (0.00 – 1.00)	2 (0 – 4)
Semi-Permanent	1	2328	312.1	55,707	0.71	2
Permanent	10	2331.7 (±59.8)	21424.1 (±8909.7)	28650.5 (±10992.0)	0.45 (0.00 – 1.00)	2 (0 – 3)

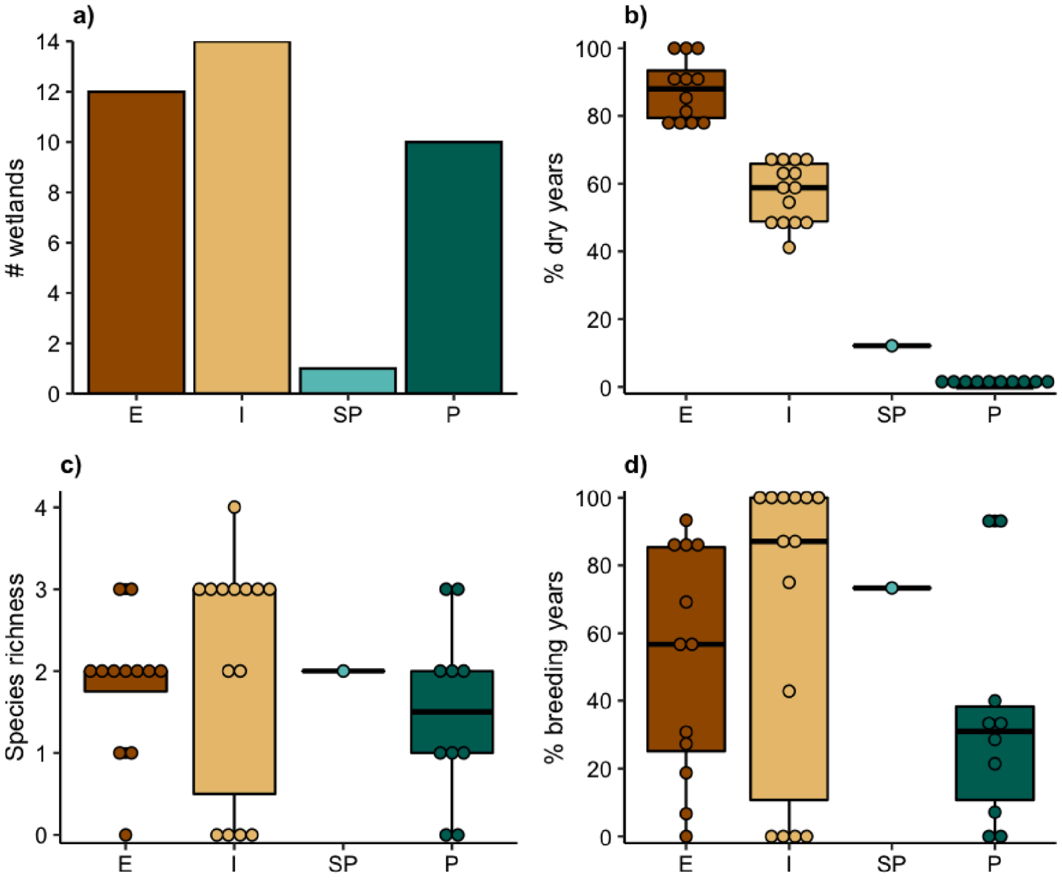

Fig. 5. Wetland hydrologic type frequencies (a) for National Park Service's long-term monitoring sites (n = 37) in Yellowstone's Northern Range. Estimated proportion of dry years (b; see methods) and linked cumulative amphibian breeding richness (c) and proportion of years with breeding (d) from visual surveys between 2005 and 2019 are summarized by wetland type.

(−0.011 ± 0.008), while the one semi-permanent wetland in this sample increased in size (0.031 ± 0.027; Fig. 6b). Differences in estimates of change among hydrologic types were not significant (F = 2.71, p = 0.061). The slope is interpreted as the annual decrease in wetland surface water area, measured in standard deviations (e.g., ephemeral wetlands decreased in size by 0.011 standard deviations per year).

3.1.3. *Runoff as a driver of wetland dynamics*

Runoff was a positive driver of early summer (i.e., June) surface water area for all 37 wetlands surveyed annually, and this effect was significant for 64.9% (n = 24) of the wetlands. Sensitivity was similar among wetland types (ephemeral wetlands: $\beta = 0.066 \pm 0.009$, $R^2 = 0.25 \pm 0.058$; intermittent wetlands: $\beta = 0.035 \pm 0.006$, $R^2 = 0.14 \pm 0.038$; semi-permanent: $\beta = 0.066$, $R^2 = 0.30$, n = 1; and permanent wetlands: $\beta = 0.060 \pm 0.007$, $R^2 = 0.31 \pm 0.059$; Fig. 6c), although runoff had a significantly weaker effect on intermittent wetlands than ephemeral ($p = 0.024$). The pivot points were also similar and did not differ significantly between wetland hydrologic types (F = 1.049, p = 0.38): the mean pivot point was 24.6 cm (SE = 5.28) of runoff for ephemeral wetlands, 35.7 cm (SE = 7.20) for intermittent, and 36.3 cm (SE = 7.83) for permanent wetlands (Fig. 6d). Half of the established long-term monitoring sites had a calculated pivot point of 27.8 cm of runoff or less, and 95% had a pivot point of 59.8 cm or less.

3.2. *NWI-mapped Northern Range wetlands*

3.2.1. *Categorization of hydrologic regimes*

From the 427 NWI-mapped wetlands we analyzed across the NR, 21.3% (n = 91) were classified as ephemeral, 36.5% (n = 156) intermittent, 15.7% (n = 67) semi-permanent, and 26.5% (n = 113) permanent (Table 2). Wetland surface water area increased from ephemeral < intermittent < semi-permanent < permanent when measured as both mean May 15 to October 15 size and the 95th quantile, although this difference was only significant between permanent wetlands and all other hydrologic types ($p < 0.1$). Permanent wetland surface water area was several-fold larger than other wetland types

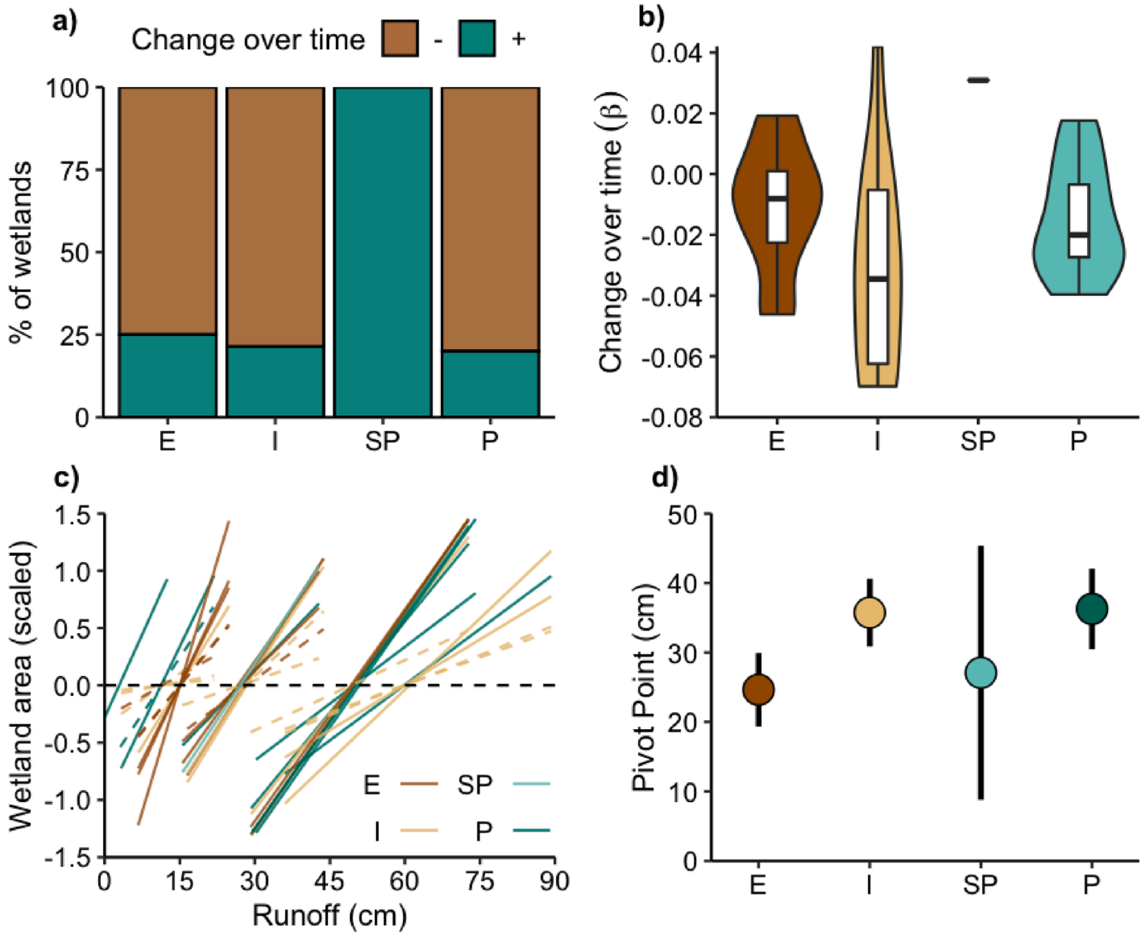

Fig. 6. Changes to National Park Service's long-term monitoring wetlands' (n = 37) surface water area over time and sensitivity to runoff. (a) The proportion of wetlands of each hydrologic type that exhibited an increase or decrease in average May 15 to October 15 surface water area from 1984 to 2018. Note that there is only one semi-permanent wetland in this sample. E = ephemeral, I = intermittent, SP = semi-permanent, P = permanent. (b) The distribution of coefficients representing the amount and direction of change in surface water area over time for wetlands in each hydrologic group. Wetland surface water area was scaled to have a mean of zero and standard deviation of one. (c) Sensitivity of scaled June wetland surface water area across water year runoff for all linear models. Solid lines represent significant runoff effects, and dashed lines are non-significant effects. Predictions were made across the range of observed runoff values for each wetland. (d) Calculated runoff pivot points for each hydrologic type. Bars represent standard error.

Table 2
Summary of U.S. Fish and Wildlife Service National Wetland Inventory (NWI) wetland hydrologic types for palustrine and lacustrine wetlands across the Northern Range. The number of wetlands (N), grouping mean of the individual wetland elevation and mean surface water area by hydrologic regime (Mean, μ [± SE]), and mean of the 95th quantile (95th Q, μ [± SE]) surface water area for all wetland hydrologic regimes.

Wetland Type	N	Mean Area (m^2)	95th Q Area (m^2)	Elevation (m)
Ephemeral	91	401 (±217)	1693 (±932)	1997.8 (±38.5)
Intermittent	156	1958 (±279)	5181 (±818)	2158.0 (±26.7)
Semi-Permanent	67	3746 (±1072)	6906 (±2045)	2221.4 (±41.3)
Permanent	113	21,544 (±7164)	26,942 (±8167)	2187.0 (±27.1)

(Table 2) and this classification of habitats also included lacustrine wetlands which are typically deeper than palustrine types.

3.2.2. *Surface water trends over time*

The majority of wetlands (62.3%, n = 266) experienced a decrease in surface water area across the study period (Fig. 7a), although this decline was only significant for 23.2% of wetlands (n = 99). On average, ephemeral wetlands experienced a nominal increase in surface water area ($\mu_\beta \pm SE = 0.0032 \pm 0.004$), while intermittent (−0.011 ± 0.005), semi-permanent (−0.016 ± 0.006), and permanent (−0.015 ± 0.005) wetlands all decreased in surface water area (Fig. 7b). The change in ephemeral wetlands was significantly different from the other wetland hydrologic types (F = 5.74, p = 0.001). Wetlands that experienced increases in size were largely concentrated outside of the YNP boundary (Fig. 7c). See Appendix (Fig. A3) for an example of one such wetland and its hydroperiod.

3.2.3. *Runoff as a driver of wetland dynamics*

Runoff was a positive driver of early summer (i.e., June) surface water area for 81.2% (n = 346) of the 426 wetlands surveyed annually (Fig. 8a), and this effect was significant for 47.4% (n = 202) of the wetlands. Regardless of whether this relationship was significant, the strength of the runoff effect (Fig. 8b) was strongest for ephemeral wetlands ($\mu_\beta \pm SE\beta = 0.105 \pm 0.012$; $\mu R^2 \pm SER^2 = 0.22 \pm 0.022$), followed by intermittent (β: 0.062 ± 0.016; R^2: 0.22 ± 0.016), semi-permanent (β: 0.049 ± 0.019; R^2: 0.17 ± 0.023), and permanent (β: 0.044 ± 0.017; R^2: 0.13 ± 0.013). An ANOVA indicated that the strength of the runoff effect varied between wetland types (F = 4.95, p = 0.002; Fig. 8b), with permanent (p = 0.002), semi-permanent (p = 0.02), and intermittent (p = 0.03) wetlands all being significantly less sensitive to variations in runoff than ephemeral wetlands. Though the mean effect was overwhelmingly positive, there were wetlands that decreased in size with

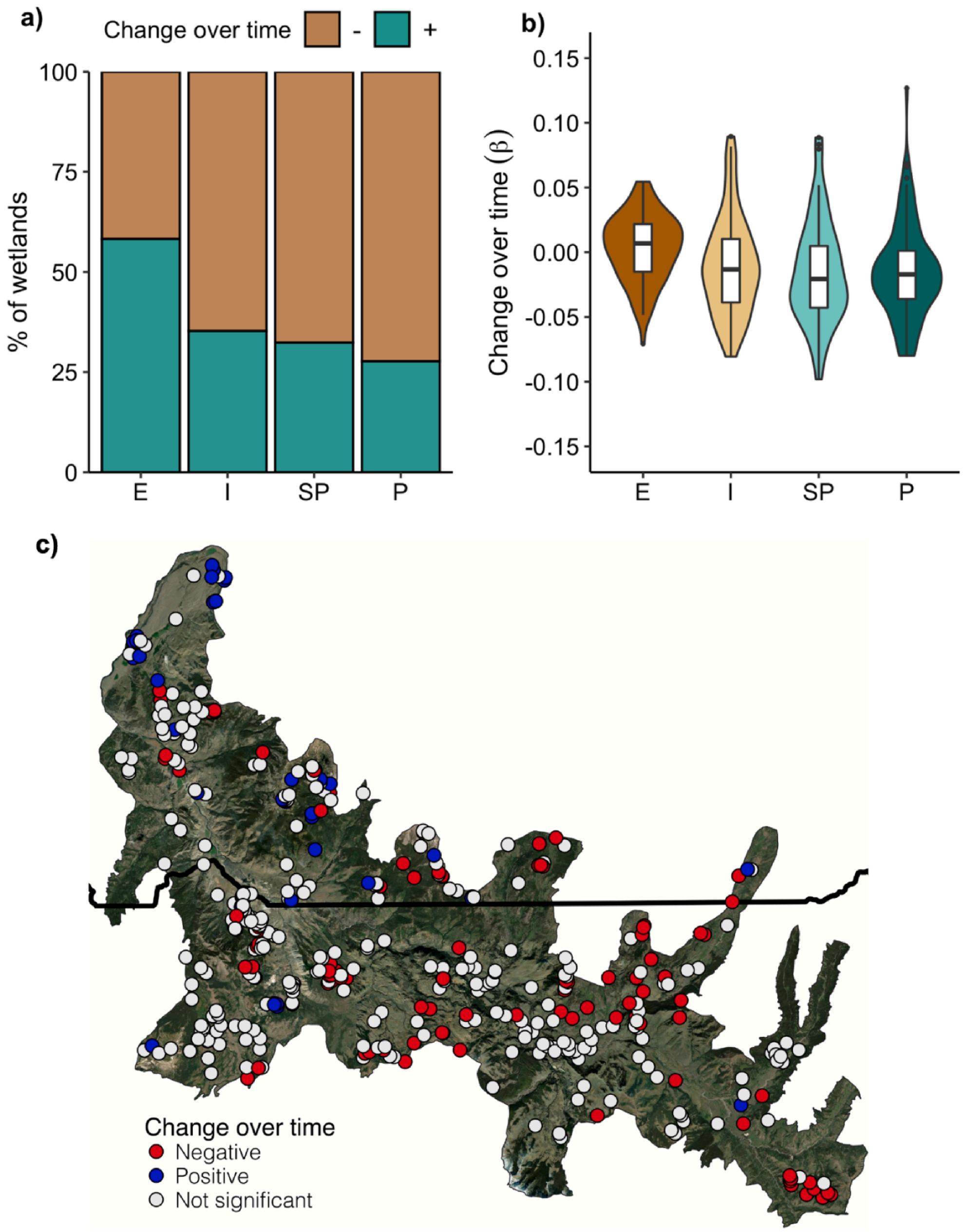

Fig. 7. Change in wetland surface water area over time across the Northern Range. (a) The percent of wetlands that have increased and decreased over time by hydrologic group. E = ephemeral, I = intermittent, SP = semi-permanent, P = permanent. (b) The distribution of coefficients representing the amount and direction of change in surface water area over time for wetlands in each hydrologic group. Wetland surface water area was scaled to have a mean of zero and standard deviation of one. (c) Spatial distribution of wetlands that have decreased (red points). increased (blue) or show no significant trend (white) in size over time. The solid black line is the Yellowstone National Park boundary.

increases in runoff (n = 80, 18.8%; Fig. 8a, c, d).

Fifty percent of wetlands had a calculated pivot point of 20.0 cm or less, and 95% had a pivot point of 62.8 cm or less (Fig. 9a). These results indicate that, when runoff is <20.0 cm, surface water area shifted from above to below the long-term average for 50% of NR wetlands. Pivot points differed significantly between hydrologic groups (F = 5.34, p = 0.001), and the rank order of mean pivot point estimates by hydrologic type were as follows: ephemeral ($\mu_\beta \pm$ SE = 17.1 ± 1.94), intermittent (23.6 ± 2.45), permanent (24.2 ± 2.61), and semi-permanent (28.7 ± 2.97; Fig. 9b).

4. Discussion

To date, the NPS's long-term monitoring program in YNP has shown that wetlands and amphibians are responsive to variations in key climate drivers and offered insight on how climate change could shape monitored wetlands and species dependent on them (Gould et al., 2019; Ray et al., 2019). Through the integration of the Landsat imagery archive, we expanded our temporal and spatial understanding of wetlands in YNP's NR in important ways. First, the Landsat archive offered multiple observations of wetlands each year, enabling characterizations of seasonal variation in wetland area over a 35-year time series that extended our monitoring record backwards by nearly two decades. This information shed light on effects of the historic, multi-year drought (Heeter et al., 2021) that occurred in the early 2000s and led to observed declines in wetland area across the NR (McMenamin et al., 2008; Schook and Cooper, 2014). This drought also preceded the lowest estimates of tiger salamander occupancy in our monitoring time series (Ray et al., 2016) and offers important clues on the possible manifestations of drought to one of the NR's most common amphibian species.

Using this more complete understanding of wetland dynamics, we were able to categorize the hydrologic types (i.e., ephemeral, intermittent, semi-permanent, and permanent) of wetlands that comprise our sample frame and then apply these same approaches to 'monitor' wetlands outside the boundaries of our randomly selected catchments to the entirety of the NR. All hydrologic types outside of the NPS's monitoring

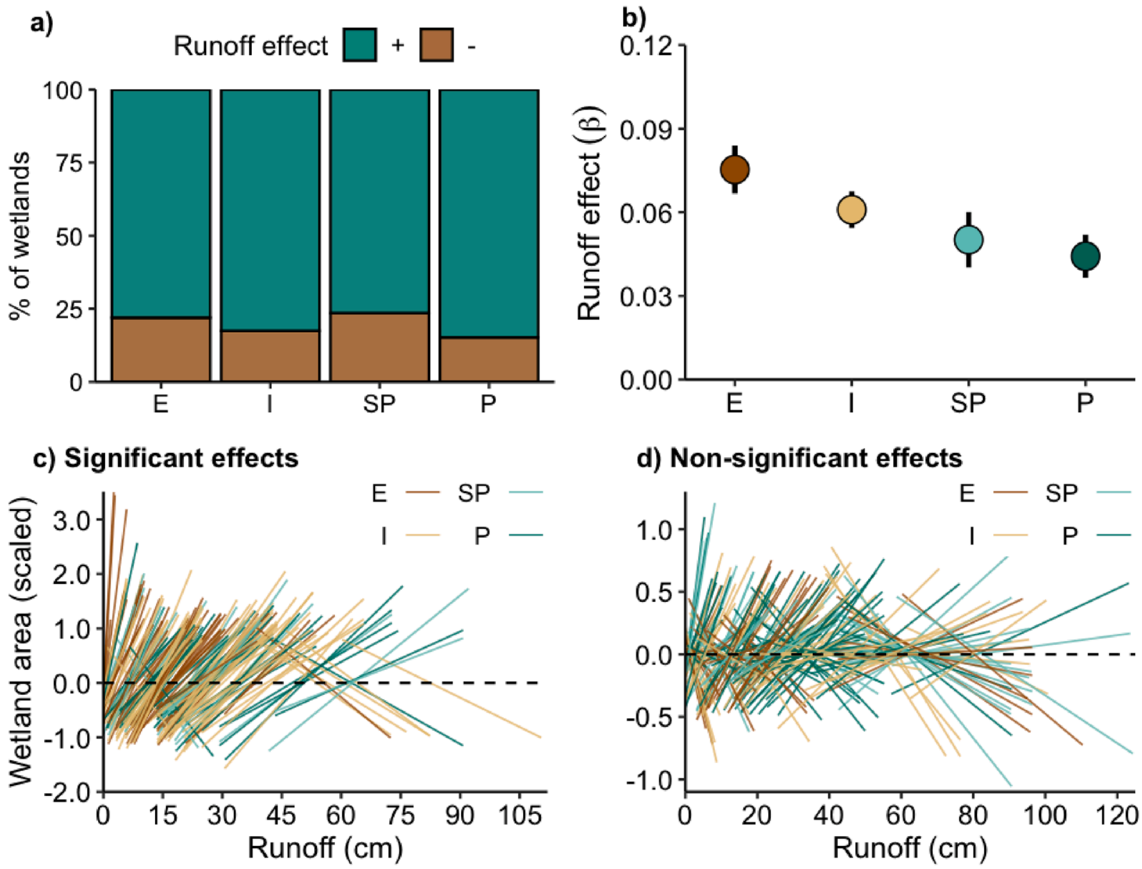

Fig. 8. Strength of water year runoff as a driver of change in June surface water area for wetlands across the Northern Range. (a) The proportion of wetlands of each hydrologic type that exhibited an increase or decrease in June surface water area with increasing runoff. E = ephemeral, I = intermittent, SP = semi-permanent, P = permanent. (b) Mean runoff effect for each hydrologic type. Bars represent the standard error. Slope is interpreted as the change in June surface water area (measured as standard deviations) with a 1-cm increase in runoff. (c) Sensitivity of scaled June wetland surface water area across water year runoff for all significant ($p < 0.1$) linear models. Wetland surface water area estimates were made across the range of observed runoff values for each wetland. Lines are colored by hydrologic type. The dashed line at zero represents the mean area for each wetland. (d) Sensitivity of scaled June wetland surface water area across water year runoff for all non-significant ($p > 0.1$) linear models.

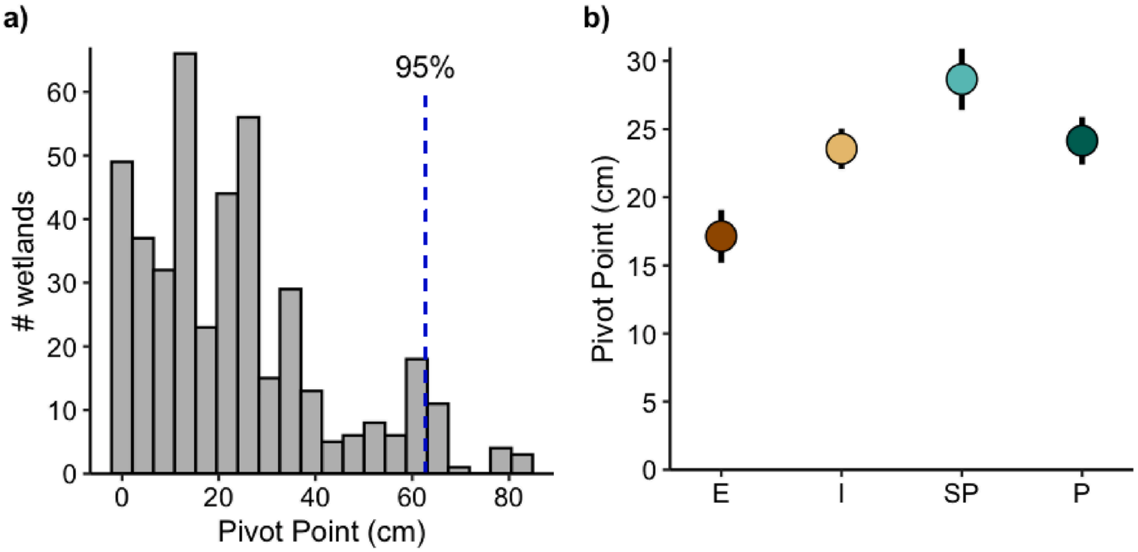

Fig. 9. Runoff pivot points for Northern Range NWI-mapped wetlands (n = 426). (a) Frequency distribution of calculated pivot points, with runoff in cm. The blue dashed line represents the 95th percentile (62.8 cm water year runoff). (b) Mean pivot point by wetland type, with standard errors (bars).

program's sample frame had an average elevation that was considerably lower (approx. 100 to 200 m) than these same types in our monitoring catchments within YNP. In addition, the NWI-mapped wetlands across the NR were disproportionately classified as intermittent using the SMA approach; however, ephemeral and intermittent wetland types are nearly equally represented in our sample frame.

Consistent with the work of others (see McCaffery et al., 2014 as an example), our ground-based monitoring showed that amphibian breeding at wetlands span the continuum of hydrologic types (from ephemeral to permanent). While some species experience higher rates of survival and production in wetlands of a particular hydrologic regime (see Karraker and Gibbs 2009; Richter et al., 2003; Semlitsch, 1987; Zero and Murphy, 2016), amphibian use of a range of wetland hydrologic types is thought to stabilize recruitment in populations that experience regular, meteorologically driven fluctuations in hydrologic conditions (McCaffery et al., 2014; Whiteman and Wissinger, 2005).

Using SMA modeled wetland surface water areas, most NR wetlands (ground-based long-term monitoring sites [75%] and NWI-mapped [62%]) exhibited declines in area between 1984 and 2018. Declines at long-term monitoring sites were steeper for ephemeral and intermittent hydrologic types when compared to those detected across the NR. While declining trends predominated in both sets of wetlands evaluated, work by Schook and Cooper (2014), and further demonstrated here, documented considerable variation in individual wetland area trends. Wetlands that experienced expansion (Fig. A3 as an example) or showed no measurable changes in surface water area may be disproportionately maintained by groundwater (Bardecki, 1991) and recharged through slower moving subsurface flow paths (Schook and Cooper, 2014). Information on subsurface flow paths is invisible to satellites, but variations in surface water area across the sample frame indicate that these subsurface hydrologic connections are not insignificant for maintaining the hydroperiods of isolated NR wetlands and that timescales of such connections are longer than for runoff generated surface flows that were evaluated here.

Snowmelt runoff has been linked to changes to wetland surface water area in YNP (Ray et al., 2019) and there is good evidence that snowpacks across the NR have declined since the 1960s (Tercek et al., 2015). In addition, forecasts for YNP indicate that snowpack declines are expected to be widespread over the next century (Tercek et al., 2016). Here, we showed that snowmelt runoff was an important driver of June wetland surface water area for nearly half of the NR wetlands evaluated. Wetlands supported by lower amounts of snowmelt runoff were most sensitive (i.e., had steeper slopes) to changes in runoff (Fig. 6c and Fig. 8c). While this effect was less obvious from our small sample size of long-term monitoring sites, the pattern of sensitivity becomes apparent using the larger sample size of NWI-mapped wetlands across the NR (Fig. 8c). The effect of runoff on wetlands described here is similarly variable across regions of YNP and neighboring GTNP, but runoff is associated with the probability of wetland drying across both park units (Ray et al., 2019). Amphibian breeding dynamics are also driven by variations in runoff. For example, Columbia spotted frog breeding persistence increases with increased runoff particularly in deeper wetlands (Gould et. al., 2019; Ray et al., 2016). In the NR, elevated runoff is also strongly associated with recurrence of tiger salamander breeding at previously dry breeding sites (see 4007-3 as an example).

4.1. Leveraging remote sensing datasets

The application of remote sensing methodologies has transformed how scientists map and monitor large landscapes (Wright and Gallant, 2007; Halabisky et al., 2016; Kissel et al., 2020; Pasquarella et al., 2016). The SMA approaches employed here expanded our work and inference severalfold from small clusters of wetlands contained within mapped catchments to the entire NR landscape. The expanded spatial coverage and application of SMA supported an evaluation of the representativeness of long-term monitoring sites (size, elevation, sensitivity, and hydrologic type) to the greater population of wetlands in this region. Notably, ephemeral wetlands appear to be overrepresented in our sample frame relative to their proportional occurrence across the NR. This overrepresentation may exist because our ground-based surveys may enable a more comprehensive canvassing of monitored catchments, including forested regions that are known to obscure remote sensing-based monitoring approaches (Halabisky et al., 2016; Wright and Gallant, 2007). Ground-based surveys may also facilitate detection of small water bodies documented as habitat for amphibians but that are dramatically smaller than a Landsat pixel (Sall et al., 2021). In addition, our reliance on NWI-mapped palustrine wetlands and lakes for the application of SMA likely eliminated potential wetland habitat that was included in our initial ground-based canvassing of catchments that included additional NWI wetland types. Finally, higher elevation regions of our sample frame are dominated by coniferous forest. Forests cast shadows that have a similar spectral signature to water (Halabisky et al., 2016), complicating our understanding of wetland surface water area, their trends, and association with runoff. Regardless, this work generated insight that will facilitate discussions on how to better represent wetland types in our monitoring program available to amphibians and representative of the frequency and distribution of wetland types across the NR.

The seasonal observations available from Landsat imagery provided at least coarse estimates of the duration of time water was present in a wetland each year. This ability to define hydroperiods is key to understanding the suitability of individual wetlands for amphibians and other wetland-dependent species (Karraker and Gibbs, 2009; McCaffery et al., 2014; Ryan et al., 2014; Zero and Murphy, 2016). Amphibians in YNP vary in their developmental periods; Columbia spotted frogs and boreal chorus frogs require standing water for 2 to 4 months to reach metamorphosis. While duration of flooding needed by individuals likely varies as a function of water temperatures and water availability (Székely et al., 2017), the larval period for both species requires multiple months of inundation. Tiger salamanders are unique in their use of alternative (paedomorphic) phenotypes to exploit habitats that vary in their hydrologic permanence. This phenotypic plasticity is dependent on more permanent water, as this species sometimes overwinters for one or more years in its larval form (Koch and Peterson, 1995). During a severe, multi-year drought of the early 2000s, NR wetlands with paedomorphic salamanders abruptly dried. Rapid drying stranded individuals present and confirmed that a relatively rapid transition of wetlands from a permanent or semi-permanent to a more ephemeral hydrologic state is possible (McMenamin et al., 2008).

Here we used SMA to reconstruct the flooding and drying trends of individual wetlands through time. While other remote sensing techniques have been used to successfully characterize wetland surface water trends (Normalized Difference Water Index, Dynamic Surface Water Extent, and European Commission's Joint Research Centre Global Surface Water products as examples), our case study demonstrates how time series data from satellite images can be leveraged for the purposes of monitoring of individual wetlands of high conservation value to monitoring all isolated, palustrine wetlands across a landscape. The selection of the optimal remote sensing method and satellite sensor depends on several factors, such as the spectral, temporal, and spatial resolution of the habitat of interest and the magnitude of changes within that habitat that is ecologically meaningful (Lechner et al., 2020).

We selected SMA because it provides sub-pixel estimates of surface water area with high accuracy for our study area and habitat of interest. We found estimates of surface water area easier to understand and validate than more commonly used spectral indices, such as the Normalized Difference Water Index (NDWI). While SMA allowed us to reconstruct surface water area estimates of wetlands through time it has several limitations. SMA works best in areas with high contrast where the landcover features are spectrally unique. Dark features that are spectrally similar to water such as shadows from trees and dark substrate can overestimate SMA modeled estimates of water. Wetlands with floating or submerged vegetation in standing water will underestimate surface water area. Shallow water, sediment, and turbid water are spectrally different from deep clear water, which was used for our SMA model, and therefore they too represent a potential source of error. Finally, another limitation of SMA is that it requires knowledge of the landscape and the selection of pure pixels that represent the landcover features of interest, which may not always be present within a landscape (Halabisky et al., 2016).

The wetlands in our study area were generally small in size and required an approach that estimated surface water extent at the sub-pixel scale. For larger wetlands, existing dynamic surface water datasets that classify pixels as water or not water may be suitable to detect changes in surface water through time (Jones, 2019; Mueller et al., 2016; Pekel et al., 2016). For the United States, the United States Geological Survey operationally generates the Dynamic Surface Water Extent or 'DSWE' as part of the Landsat Level 3 Collection, that includes additional classes, such as 'potential wetland', that may pick up partially inundated pixels better than other hard water classifiers (Jones, 2015; Jones, 2019).

SMA supports seasonal and multi-year estimates of flooding duration in individual wetlands that are meaningful to understanding their suitability to different amphibian species and phenotypes, but our application of this approach lacks information on other attributes of ponds (e.g., depth and vegetative cover) that may be important for amphibian breeding. Both spotted frogs and tiger salamander breeding is related to maximum pond depth and chorus frog breeding is related to extent of vegetative cover (Gould et al., 2019; Ray et al., 2016). Other remote sensing tools (e.g., LiDAR) might therefore provide additional clues on the suitability of the habitat to amphibians that would be complementary to the work described (Koma et al., 2021). Finally, the Landsat archive provides a long-term continual time-series of satellite imagery reaching back decades, but in the last ten years several new satellites have been launched and can be used to increase the frequency of observations. Sentinel-2, launched in 2015, provides increased frequency and higher resolution images for monitoring wetland change (Kaplan and Avdan, 2017; Slagter et al., 2020). Synthetic Aperture Radar (SAR), which is less impacted by atmospheric conditions, as well as high-resolution commercial satellite imagery (e.g., Planet imagery), can also increase observation frequency (Endo et al., 2020; Kuhn et al., 2020). There is active research in the development and application of methods similar to SMA that measure changes at sub-pixel scales that range from simple indices (e.g., NDWI) to complex machine learning methods (Devries et al., 2017; Huang et al., 2018).

Remote sensing has strengthened our ability to inventory and monitor wetlands across large remote regions (Gallant, 2015). In YNP, remote sensing approaches described here (see Appendix) and elsewhere (Wright and Gallant, 2007) offer quantifiable advantages to inventorying wetlands over increasingly dated wetland inventories (i.e., NWI). Still, management-relevant wetland monitoring capabilities in YNP will require the integration of remote sensing technologies and ground-based field assessments. The former offers advantages in our ability to detect and characterize changes in wetland extent across large landscapes, and the latter provides essential evidence on changes in wetland condition and use by wetland-dependent species. For this reason, Wright and Gallant (2007) recommended the establishment of permanent wetland plots in YNP that could be used to calibrate and field-verify remote sensing summaries of wetlands. Today, annual field visits have revealed details and manifestations of wetland conditions that are simply unavailable from remotely sensed data. As interest in the ecological services of wetlands grows (Cohen et al., 2016), so too will the approaches to leverage and fuse datasets that enrich monitoring of wetlands and wetland-dependent species. Here, we offer a framework for documenting the hydrobiological dynamics of individual wetlands that also shines a light on the idiosyncratic responses of wetlands across large landscapes. Further, information generated here will be critical to developing and implementing conservation plans that promote wetland resilience and advance amphibian conservation at scales ranging from ponds to landscapes.

5. Conclusions

Wetlands are uniquely responsive to variations in climate drivers, and there is a long list of species dependent on them for some portion of their life cycle. Given their prominent role in supporting biodiversity, documented variations in the wetland surface water area have caught the attention of land managers and the public (Cohen et al., 2016). Across the western U.S., studies have documented climate-induced declines in wetland surface water area and described the peculiarities of wetland responses across the landscape (Halabisky et al., 2016; Kissel et al., 2020; Schook and Cooper, 2014). Here, we demonstrate how the integration of multidisciplinary approaches allowed an ongoing ground-based monitoring program to make the leap from clusters of ponds to landscapes. This case study also highlights how integration of physical, biological (amphibian), and meteorological datasets can strengthen our understanding of the drivers and implications of change. Documenting past changes to wetland hydroperiods and understanding the drivers and manifestations of change will help inform the public about ongoing change and managers who are developing climate adaptation strategies.

CRediT authorship contribution statement

Elaine M. Brice: Data curation, Methodology, Formal analysis, Writing – original draft, Writing – review & editing, Visualization. **Meghan Halabisky:** Conceptualization, Data curation, Formal analysis, Writing – original draft, Writing – review & editing, Visualization. **Andrew M. Ray:** Data curation, Conceptualization, Writing – original draft, Writing – review & editing, Visualization, Supervision, Project administration.

Declaration of Competing Interest

The authors declare that they have no known competing financial interests or personal relationships that could have appeared to influence the work reported in this paper.

Acknowledgements

We acknowledge the efforts of current and past field crews that collectively produced the ground-based data and Mike Tercek for the water balance data available for this analysis. We recognize Steve Corn and Chuck Peterson for their leadership in conceiving and establishing the long-term amphibian and wetland monitoring program in YNP. We thank Maureen Ryan, David Thoma, Kristin Legg, and two anonymous reviewers for comments on an earlier version of this manuscript. Amphibian photos are courtesy of Chuck Peterson. We acknowledge support from the U.S. National Science Foundation (DGE-1633756), and the S.J. and Jessie E. Quinney Doctoral Fellowship.

Funding

This work was supported by the National Park Service and National Science Foundation (DGE-1633756).

Appendix A. Supplementary data

Supplementary data to this article can be found online at https://doi.org/10.1016/j.ecolind.2022.108559.

References:

Bardecki, M.J., 1991. Wetlands and climate change: a speculative review. Can. Water Resour. J. 16 (1), 9–22.

Casanova, M.T., Brock, M.A., 2000. How do depth, duration and frequency of flooding influence the establishment of wetland plant communities? Plant Ecol. 147, 237–250.

Case, M.J., Lawler, J.J., Tomasevic, J.A., 2015. Relative sensitivity to climate change of species in northwestern North America. Biol. Conserv. 187, 127–133.

Cohen, M.J., Creed, I.F., Alexander, L., Basu, N.B., Calhoun, A.J.K., Craft, C., D'Amico, E., DeKeyser, E., Fowler, L., Golden, H.E., Jawitz, J.W., Kalla, P., Kirkman, L.K., Lane, C.R., Lang, M., Leibowitz, S.G., Lewis, D.B., Marton, J., McLaughlin, D.L., Mushet, D.M., Raanan-Kiperwas, H., Rains, M.C., Smith, L., Walls, S.C., 2016. Do geographically isolated wetlands influence landscape functions? Proc. Natl. Acad. Sci. 113, 1978–1986.

Collen, B., Whitton, F., Dyer, E.E., Bailie, J.E.M., Cumberlidge, N., Darwall, W.R.T., Pollock, C., Richman, N.I., Soulsby, A.-M., Böhm, M., 2013. Global patterns of freshwater species diversity, threat, and endism. Global Ecol. Biogeogr. 23, 40–51.

L.M. Cowardin V. Carter F.C. Golet E.T. LaRoe Classification of wetlands and deepwater habitats of the United States. U.S. Department of the Interior, Office of Biological Services, U.S 1979 USA.

Darrah, Sarah E., Shennan-Farpón, Yara, Loh, Jonathan, Davidson, Nick C., Finlayson, C. Max, Gardner, Royal C., Walpole, Matt J., 2019. Improvements to the Wetland Extent Trends (WET) index as a tool for monitoring natural and human-made wetlands. Ecol. Indic. 99, 294–298.

DeVries, B., Huang, C., Lang, M.W., Jones, J.W., Huang, W., Creed, I.F., Carroll, M.L., 2017. Automated quantification of surface water inundation in wetlands using optical satellite imagery. Remote Sens. 2017 (9), 807. https://doi:10.3390/rs9080807.

Endo, Y., Halabisky, M., Moskal, L.M., Koshimura, S., 2020. Wetland surface water detection from SAR images using Multi-Angle/Temporal Gaussian Process Regression. Remote Sensing 12 (11), 1756. https://doi:10.3390/rs12111756.

Fancy, S.G., Gross, J.E., Carter, S.L., 2009. Monitoring the condition of natural resources in US national parks. Environ. Monit. Assess. 151 (1-4), 161–174.

Figel, Joe J., Botero-Cañola, Sebastián, Forero-Medina, German, Sánchez-Londoño, Juan David, Valenzuela, Leonor, Noss, Reed F., Goodrich, John, 2019. Wetlands are keystone habitats for jaguars in an intercontinental biodiversity hotspot. PLoS ONE 14 (9), e0221705. https://doi.org/10.1371/journal.pone.022170510.1371/journal.pone.0221705.g00110.1371/journal.pone.0221705.g00210.1371/journal.pone.0221705.g00310.1371/journal.pone.0221705.g00410.1371/journal.pone.0221705.t00110.1371/journal.pone.0221705.t00210.1371/journal.pone.0221705.t00310.1371/journal.pone.0221705.t00410.1371/journal.pone.0221705.t00510.1371/journal.pone.0221705.s00110.1371/journal.pone.0221705.s00210.1371/journal.pone.0221705.s00310.1371/journal.pone.0221705.s004.

Gallant, Alisa, 2015. The challenges of remote monitoring of wetlands. Remote Sens. 7 (8), 10938–10950.

Gould, W.R., Patla, D.A., Daley, R., Corn, P.S., Hossack, B.R., Bennetts, R., Peterson, C.R., 2012. Estimating occupancy in large landscapes: evaluation of amphibian monitoring in the Greater Yellowstone Ecosystem. Wetlands 32, 379–389. https://doi.org/10.1007/s13157-012-0273-0.

Gould, William R., Ray, Andrew M., Bailey, Larissa L., Thoma, David, Daley, Rob, Legg, Kristin, 2019. Multistate occupancy modeling improves understanding of amphibian breeding dynamics in the Greater Yellowstone Area. Ecol. Appl. 29 (1) https://doi.org/10.1002/eap.2019.29.issue-110.1002/eap.1825.

Halabisky, Meghan, Moskal, L. Monika, Gillespie, Alan, Hannam, Michael, 2016. Reconstructing semi-arid wetland surface water dynamics through spectral mixture analysis of a time series of Landsat satellite images (1984–2011). Remote Sens. Environ. 177, 171–183.

K.J. Heeter M.L. Rochner G.L. Harley Summer air temperature for the Greater Yellowstone Ecoregion (770–2019 CE) over 1,250 years Geophys. Res. Lett. 48 2021 e2020GL092269.

Hollander, M., Wolfe, D.A., 1999. Nonparametric Statistical Methods, Second Edition. Wiley, New York, New York, USA.

Hossack, Blake R., Gould, William R., Patla, Debra A., Muths, Erin, Daley, Rob, Legg, Kristin, Corn, Paul Stephen, 2015. Trends in Rocky Mountain amphibians and the role of beaver as a keystone species. Biol. Cons. 187, 260–269.

Hossack, Blake R., Honeycutt, R. Ken, Sigafus, Brent H., Muths, Erin, Crawford, Catherine L., Jones, Thomas R., Sorensen, Jeff A., Rorabaugh, James C., Chambert, Thierry, 2017. Informing recovery in a human-transformed landscape: Drought-mediated coexistence alters population trends of an imperiled salamander and invasive predators. Biol. Cons. 209, 377–394.

Huang, Chang, Chen, Yun, Zhang, Shiqiang, Wu, Jianping, 2018. Detecting, extracting, and monitoring surface water from space using optical sensors: a review Rev. Geophys. 56 (2), 333–360.

IUCN 2021. The IUCN Red List of Threatened Species. Version 2021-1. https://www.iucnredlist.org. (accessed 9 August 2021).

Jones, John, 2015. Efficient wetland surface water detection and monitoring via Landsat: Comparison with in situ data from the Everglades Depth Estimation Network. Remote Sens. 7 (9), 12503–12538.

Jones, J.W., 2019. Improved automated detection of subpixel-scale inundation – revised Dynamic Surface Water Extent (DSWE) partial surface water tests. Remote Sens. 11, 374. https://doi.org/10.3390/rs11040374.

Kaplan, G., Avdan, U., 2017. Mapping and monitoring wetlands using Sentinel-2 satellite imagery ISPRS Ann. Photogramm. Remote Sens. Spat. Inf. Sci. 4, 271–277.

Karraker, Nancy E., Gibbs, James P., 2009. Amphibian production in forested landscapes in relation to wetland hydroperiod: a case study of vernal pools and beaver ponds. Biol. Cons. 142 (10), 2293–2302.

Kissel, Amanda M, Halabisky, Meghan, Scherer, Rick D, Ryan, Maureen E, Hansen, Eric C, 2020. Expanding wetland hydroperiod data via satellite imagery for ecological applications. Front. Ecol. Environ. 18 (8), 432–438.

Koch, E.D., Peterson, C.R., 1995. Amphibians & reptiles of Yellowstone and Grand Teton National Parks. University of Utah Press, Salt Lake City, Utah, USA.

Koma, Zsófia, Zlinszky, András, Bekő, László, Burai, Péter, Seijmonsbergen, Arie C., Kissling, W. Daniel, 2021. Quantifying 3D vegetation structure in wetlands using differently measured airborne laser scanning data. Ecol. Indic. 127, 107752. https://doi.org/10.1016/j.ecolind.2021.107752.

Kuhn, C., Bogard, M., Johnston, S.E., John, A., Vermote, E., Spencer, R., Dornblaser, M., Wickland, K., Striegl, R., Butman, D., 2020. Satellite and airborne remote sensing of gross primary productivity in boreal Alaskan lakes. Environ. Res. Lett. 15, 105001. https://doi: 10.1088/1748-9326/aba46f.

Lechner, Alex M., Foody, Giles M., Boyd, Doreen S., 2020. Applications in remote sensing to forest ecology and management. One Earth 2 (5), 405–412.

Lee, Se-Yeun, Ryan, Maureen E., Hamlet, Alan F., Palen, Wendy J., Lawler, Joshua J., Halabisky, Meghan, Richardson, Curtis J., 2015. Projecting the hydrologic impacts of climate change on montane wetlands. PLoS ONE 10 (9), e0136385. https://doi.org/10.1371/journal.pone.013638510.1371/journal.pone.0136385.g00110.1371/journal.pone.0136385.g00210.1371/journal.pone.0136385.g00310.1371/journal.pone.0136385.g00410.1371/journal.pone.0136385.g00510.1371/journal.pone.0136385.g00610.1371/journal.pone.0136385.g00710.1371/journal.pone.0136385.g00810.1371/journal.pone.0136385.g00910.1371/journal.pone.0136385.g01010.1371/journal.pone.0136385.t00110.1371/journal.pone.0136385.t00210.1371/journal.pone.0136385.s00110.1371/journal.pone.0136385.s00210.1371/journal.pone.0136385.s00310.1371/journal.pone.0136385.s00410.1371/journal.pone.0136385.s00510.1371/journal.pone.0136385.s00610.1371/journal.pone.0136385.s00710.1371/journal.pone.0136385.s008.

Levandowski, M.L., Litt, A.R., McKenna, M.F., Burson, S., Legg, K.L., 2021. Multi-method biodiversity assessments from wetlands in Grand Teton National Park. Ecol. Indic. 131, 108205. https://doi.org/10.1016/j.ecolind.2021.108205.

Locky, D.A., 2016. Wetlands as keystone ecosystems: conservation cornerstones in dynamically-changing landscapes. Proc. 15th Int. PEAT Congress 1–2, 248–252.

J.G. Masek E.F. Vermote N. Saleous R. Wolfe F.G. Hall F. Huemmrich F. Gao J. Kutler T. K. Lim LEDAPS Landsat Calibration 2012 ORNL DAAC, Oak Ridge, Tennessee, USA Reflectance, Atmospheric Correction Preprocessing Code 10.3334/ORNLDAAC/1080.

Matthews, J., 2010. Anthropogenic climate change impacts on ponds: a thermal mass perspective. BioRisk 5, 193–209.

McCaffery, Rebecca M., Eby, Lisa A., Maxell, Bryce A., Corn, Paul Stephen, 2014. Breeding site heterogeneity reduces variability in frog recruitment and population dynamics. Biol. Conserv. 170, 169–176.

McIntyre, N.E., Liu, G., Gorzo, J., Wright, C.K., Guntenspergen, G.R., Schwartz, F., 2019. Simulating the effects of climate variability on waterbodies and wetland-dependent birds in the Prairie Pothole Region. Ecosphere 10 (4). https://doi.org/10.1002/ecs2.2019.10.issue-410.1002/ecs2.2711.

McMenamin, S.K., Hadly, E.A., Wright, C.K., 2008. Climatic change and wetland desiccation cause amphibian decline in Yellowstone National Park. Proc. Natl. Acad. Sci. 105 (44), 16988–16993.

Mosley, Jeffrey C., Fidel, Joseph, Hunter, Harold E., Husby, Peter O., Kay, Charles E., Mundinger, John G., Yonk, Ryan M., 2018. An ecological assessment of the Northern Yellowstone Range: introduction to the special issue. Rangelands 40 (6), 173–176.

Mueller, N., Lewis, A., Roberts, D., Ring, S., Melrose, R., Sixsmith, J., Lymburner, L., McIntyre, A., Tan, P., Curnow, S., Ip, A., 2016. Water observations from space: mapping surface water from 25 years of Landsat imagery across Australia. Remote Sens Environ 174, 341–352.

Muths, E., Chambert, T., Schmidt, B.R., Miller, D.A.W., Hossack, B.R., Joly, P., Grolet, O., Green, D.M., Pilliod, D.S., Cheylan, M., Fisher, R.N., McCaffery, R.M., Adams, M.J., Palen, W.J., Arntzen, J.W., Garwood, J., Fellers, G., Thirion, J.-M., Besnard, A., Campbell Grant, E.H., 2017. Heterogeneous responses of temperate-zone amphibian populations to climate change complicates conservation planning. Sci. Rep. 7, 17102.

Pasquarella, Valerie J., Holden, Christopher E., Kaufman, Les, Woodcock, Curtis E., Nagendra, Harini, He, Kate, 2016. From imagery to ecology: leveraging time series of all available Landsat observations to map and monitor ecosystem state and dynamics. Remote Sens. Ecol. Conserv. 2 (3), 152–170.

Pekel, Jean-François, Cottam, Andrew, Gorelick, Noel, Belward, Alan S., 2016. High-resolution mapping of global surface water and its long-term changes. Nature 540 (7633), 418–422.

Ray, A.M., Gould, W., Hossack, B., Sepulveda, A., Thoma, D., Patla, D., Daley, R., Al-Chokachy, R., 2016. Influence of climate drivers on extinction and colonization rates of wetland-dependent species. Ecosphere 7, e01409.

Ray, Andrew M., Sepulveda, Adam J., Irvine, Kathryn M., Wilmoth, Siri K.C., Thoma, David P., Patla, Debra A., 2019. Wetland drying linked to variations in snowmelt runoff across Grand Teton and Yellowstone national parks. Sci. Total Environ. 666, 1188–1197.

Richter, Stephen C., Young, Jeanne E., Johnson, Glen N., Seigel, Richard A., 2003. Stochastic variation in reproductive success of a rare frog, Rana sevosa: implications for conservation, and for monitoring amphibian populations. Biol. Conserv. 111 (2), 171–177.

RICHTER-BOIX, ALEX, LLORENTE, GUSTAVO A., MONTORI, ALBERT, 2007. Structure and dynamics of an amphibian metacommunity in two regions. J. Anim. Ecol. 76 (3), 607–618.

Ripple, William J, Larsen, Eric J, Renkin, Roy A, Smith, Douglas W, 2001. Trophic cascades among wolves, elk, and aspen on Yellowstone National Park's northern range. Biol. Conserv. 102 (3), 227–234.

Rodhouse, Thomas J., Sergeant, Christopher J., Schweiger, E. William, 2016. Ecological monitoring and evidence-based decision making in America's National Parks: highlights of the Special Feature. Ecosphere 7 (11). https://doi.org/10.1002/ecs2.2016.7.issue-1110.1002/ecs2.1608.

Rowe, Jennifer C., Duarte, Adam, Pearl, Christopher A., McCreary, Brome, Haggerty, Patricia K., Jones, John W., Adams, Michael J., 2021. Demography of the Oregon spotted frog along a hydrologically modified river. Ecosphere 12 (6). https://doi.org/10.1002/ecs2.v12.610.1002/ecs2.3634.

Ryan, Maureen E, Palen, Wendy J, Adams, Michael J, Rochefort, Regina M, 2014. Amphibians in the climate vise: loss and restoration of resilience of montane wetland ecosystems in the western U.S. Front. Ecol. Environ. 12 (4), 232–240.

Sall, Ibrahima, Jarchow, Christopher J., Sigafus, Brent H., Eby, Lisa A., Forzley, Michael J., Hossack, Blake R., He, Kate, Zlinszky, András, 2021. Estimating inundation of small waterbodies with sub-pixel analysis of Landsat imagery: long-term trends in surface water area and evaluation of common drought indices. Remote Sens. Ecol. Conserv. 7 (1), 109–124.

Schook, Derek M., Cooper, David J., 2014. Climatic and hydrologic processes leading to wetland losses in Yellowstone National Park. USA. J. Hydrol. 510, 340–352.

Semlitsch, Raymond D., 1987. Relationship of pond drying to the reproductive success of the salamander *Ambystoma talpoideum*. Copeia 1987 (1), 61. https://doi.org/10.2307/1446038.

Slagter, Bart, Tsendbazar, Nandin-Erdene, Vollrath, Andreas, Reiche, Johannes, 2020. Mapping wetland characteristics using temporally dense Sentinel-1 and Sentinel-2 data: A case study in the St. Lucia wetlands, South Africa. Int. J. Appl. Earth Obs. 86, 102009. https://doi.org/10.1016/j.jag.2019.102009.

Snodgrass, Joel W., Komoroski, Mark J., Bryan, A. Lawrence, Burger, Joanna, 2000. Relationships among isolated wetland size, hydroperiod, and amphibian species richness: Implications for wetland regulations. Conserv. Biol. 14 (2), 414–419.

Székely, D., Denoël, M., Székely, P., Cogălniceanu, D., 2017. Pond drying cues and their effects on growth and metamorphosis in a fast-developing amphibian. J. Zool. 303 (2), 129–135.

Tarr, T.L., Baber, M.J., Babbitt, K.J., 2005. Macroinvertebrate community structure across a wetland hydroperiod gradient in southern New Hampshire. USA. Wet. Ecol. Manag. 13 (3), 321–334.

Tercek, M., Rodman, A., Thoma, D., 2015. Trends in Yellowstone's snowpack. Yellowstone Sci. 23, 20–28.

Tercek, Michael, Rodman, Ann, Añel, Juan A., 2016. Forecasts of 21st century snowpack and implications for snowmobile and snowcoach use in Yellowstone National Park. PLoS ONE 11 (7), e0159218. https://doi.org/10.1371/journal.pone.015921810.1371/journal.pone.0159218.g00110.1371/journal.pone.0159218.g00210.1371/journal.pone.0159218.g00310.1371/journal.pone.0159218.g00410.1371/journal.pone.0159218.g00510.1371/journal.pone.0159218.g00610.1371/journal.pone.0159218.g00710.1371/journal.pone.0159218.g00810.1371/journal.pone.0159218.g00910.1371/journal.pone.0159218.g01010.1371/journal.pone.0159218.g01110.1371/journal.pone.0159218.g01210.1371/journal.pone.0159218.g01310.1371/journal.pone.0159218.g01410.1371/journal.pone.0159218.g01510.1371/journal.pone.0159218.g01610.1371/journal.pone.0159218.t00110.1371/journal.pone.0159218.t00210.1371/journal.pone.0159218.t003.

Tercek, Michael T., Thoma, David, Gross, John E., Sherrill, Kirk, Kagone, Stefanie, Senay, Gabriel, Martínez-Yrízar, Angelina, 2021. Historical changes in plant water use and need in the Continental United States. PLoS ONE 16 (9), e0256586. https://doi.org/10.1371/journal.pone.025658610.1371/journal.pone.0256586.g00110.1371/journal.pone.0256586.g00210.1371/journal.pone.0256586.g00310.1371/journal.pone.0256586.g00410.1371/journal.pone.0256586.g00510.1371/journal.pone.0256586.g00610.1371/journal.pone.0256586.g00710.1371/journal.pone.0256586.g00810.1371/journal.pone.0256586.g00910.1371/journal.pone.0256586.s00110.1371/journal.pone.0256586.s00210.1371/journal.pone.0256586.s00310.1371/journal.pone.0256586.s00410.1371/journal.pone.0256586.s00510.1371/journal.pone.0256586.s00610.1371/journal.pone.0256586.s007.

Tews, J., Brose, U., Grimm, V., Tielbörger, K., Wichmann, M.C., Schwager, M., Jeltsch, F., 2004. Animal species diversity driven by habitat heterogeneity/diversity: the importance of keystone structures. J. Biogeogr. 31, 79–92.

Thoma, D., Rodman, A., Tercek, M., 2015. Water in the balance: interpreting climate change impacts using a water balance model. Yellowstone Sci. 23, 29–35.

Thoma, David P., Munson, Seth M., Witwicki, Dana L., Macinnis-Ng, Cate, 2019. Landscape pivot points and responses to water balance in national parks of the southwest US. J. Appl. Ecol. 56 (1), 157–167.

Turner, F.B., 1955. Reptiles and amphibians of Yellowstone National Park. Yellowstone National Park, Wyoming, USA.

Vermote, Eric, Justice, Chris, Claverie, Martin, Franch, Belen, 2016. Preliminary analysis of the performance of the Landsat 8/OLI land surface reflectance product. Remote Sens. Environ. 185, 46–56.

Walls, Susan C., Barichivich, William J., Brown, Mary E., Scott, David E., Hossack, Blake R., 2013. Influence of drought on salamander occupancy of isolated wetlands on the Southeastern Coastal Plain of the United States. Wetlands 33 (2), 345–354.

Wellborn, Gary A., Skelly, David K., Werner, Earl E., 1996. Mechanisms creating community structure across a freshwater habitat gradient. Ann. Rev. Ecol. Syst. 27 (1), 337–363.

Whiteman, H.H., Wissinger, S.A., 2005. Amphibian population cycles and long-term data sets. In: Lanoo, M.J. (Ed.), Conservation and status of North American amphibians. University of California Press, Berkeley, CA, USA.

Wright, Chris, Gallant, Alisa, 2007. Improved wetland remote sensing in Yellowstone National Park using classification trees to combine TM imagery and ancillary environmental data. Remote Sens. Environ. 107 (4), 582–605.

Zero, Victoria H., Murphy, Melanie A., 2016. An amphibian species of concern prefers breeding in active beaver ponds. Ecosphere 7 (5). https://doi.org/10.1002/ecs2.1330.